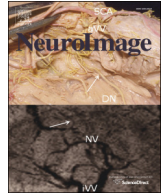




Contents lists available at ScienceDirect

NeuroImage

journal homepage: www.elsevier.com/locate/ynimg

Q2 Evidence for an anterior–posterior differentiation in the human 2 hippocampal formation revealed by meta-analytic parcellation of fMRI 3 coordinate maps: Focus on the subiculum

Q3 Henry W. Chase ^{a,*}, Mareike Clos ^{b,c}, Sofia Dibble ^d, Peter Fox ^{e,f}, Anthony A. Grace ^{a,d,g},
5 Mary L. Phillips ^a, Simon B. Eickhoff ^{b,h}

Q4 ^a Department of Psychiatry, University of Pittsburgh School of Medicine, Pittsburgh, PA, USA

7 ^b Institute of Neuroscience and Medicine (INM-1), Research Center Jülich, Germany

8 ^c Department of Systems Neuroscience, University Medical Center Hamburg-Eppendorf, Germany

9 ^d Department of Neuroscience, University of Pittsburgh, Pittsburgh, PA, USA

10 ^e Research Imaging Center, University of Texas Health Science Center San Antonio, San Antonio, TX, USA

11 ^f South Texas Veterans Administration Medical Center, San Antonio, TX, USA

12 ^g Department of Psychology, University of Pittsburgh, Pittsburgh, PA, USA

13 ^h Institute of Clinical Neuroscience and Medical Psychology, Heinrich-Heine University Düsseldorf, Germany

1 4 A R T I C L E I N F O

15 *Article history:*
16 Received 19 July 2014
17 Accepted 25 February 2015
18 Available online xxxx

19 *Keywords:*
20 fMRI
21 Subiculum
22 Meta analytic connectivity modeling
23 Resting fMRI
24 K-means clustering

A B S T R A C T

Previous studies, predominantly in experimental animals, have suggested the presence of a differentiation of 25 function across the hippocampal formation. In rodents, ventral regions are thought to be involved in emotional 26 behavior while dorsal regions mediate cognitive or spatial processes. Using a combination of modeling the co- 27 occurrence of significant activations across thousands of neuroimaging experiments and subsequent data- 28 driven clustering of these data we were able to provide evidence of distinct subregions within a region corre- 29 sponding to the human subiculum, a critical hub within the hippocampal formation. This connectivity-based 30 model consists of a bilateral anterior region, as well as separate posterior and intermediate regions on each hemi- 31 sphere. Functional connectivity assessed both by meta-analytic and resting fMRI approaches revealed that more 32 anterior regions were more strongly connected to the default mode network, and more posterior regions were 33 more strongly connected to ‘task positive’ regions. In addition, our analysis revealed that the anterior subregion 34 was functionally connected to the ventral striatum, midbrain and amygdala, a circuit that is central to models of 35 stress and motivated behavior. Analysis of a behavioral taxonomy provided evidence for a role for each subregion 36 in mnemonic processing, as well as implication of the anterior subregion in emotional and visual processing and 37 the right posterior subregion in reward processing. These findings lend support to models which posit anterior– 38 posterior differentiation of function within the human hippocampal formation and complement other early steps 39 toward a comparative (cross-species) model of the region. 40

© 2015 Published by Elsevier Inc. 41

43

44

46

Introduction

47 The hippocampal formation is crucial for mnemonic and spatial rep-
48 resentation, as well as an involvement in emotional and stress-related
49 processes. The region is made up of several independent subregions,
50 but functional specialization within the structure remains an area of
51 ongoing experimental and theoretical concern. A variety of evidence
52 supports the presence of functional specialization across a dorso-
53 ventral gradient in rodents (Fanselow and Dong, 2010). Shaped as a
54 cashew in these animals, the longitudinal axis extends in a dorsoventral

(and septotemporal) direction. Broadly, ventral regions of the hippo- 55 campal formation are often considered to play a role in emotional 56 behavior such as anxiety, whereas dorsal regions are thought to play a 57 role in cognitive factors such as spatial and mnemonic processes 58 (Bannerman et al., 2014). In primates, the hippocampal formation is 59 shaped as a ram’s horn, extending in the posterioanterior direction. 60 Consequently, the rodent ventral hippocampus is thought to corre- 61 spond to the anterior hippocampus in humans, whereas the rodent 62 dorsal hippocampus is located posterior in humans (Strange et al., 63 2014). 64

Similar evidence for differentiation of function across the region in 65 humans is perhaps sparser (Poppenk et al., 2013), partly due to the 66 technical challenges associated with experimental manipulations, neu- 67 rophysiological recordings or neuroimaging of the region. Nevertheless, 68 several fMRI studies have reported distinct patterns of activation across 69

* Corresponding author at: Western Psychiatric Institute and Clinic, Loeffler Building,
121 Meyran Avenue, Pittsburgh, PA 15213, USA. Fax: +1 412 383 8336.
E-mail address: chaseh@upmc.edu (H.W. Chase).

anterior and posterior regions of the hippocampus (e.g. [Baumann and Mattingley, 2013](#); [Hirshhorn et al., 2012](#); [Kuhn and Gallinat, 2014](#); [Nadel et al., 2013](#); [Strange et al., 1999](#); [Voets et al., 2014](#)). Another promising approach has been to examine patterns of resting functional connectivity with other structures, using for example, resting state fMRI (rsfMRI). These methods have proven to be a powerful way to investigate the communication of information across the human brain ([Van Dijk et al., 2010](#)), yielding patterns of connectivity that appear to correspond well to known neural circuits, and may reflect underlying anatomical connections ([Baria et al., 2013](#); [Damoiseaux and Greicius, 2009](#)) and functional networks. A recent resting state fMRI study described the functional connectivity of the hippocampus with perirhinal and parahippocampal regions as following an antero-posterior gradient: most posterior regions were connected to parahippocampal compared with perirhinal cortex, whereas the reverse pattern was observed in anterior regions ([Libby et al., 2012](#)). An intermediate region demonstrated no preferential connectivity. This study implied that zones of differential functional connectivity within the hippocampus may reflect the presence of different functional properties of the more anterior and more posterior portions of the region, and accorded well with anatomical properties of the region as primarily known from animal models. Another recent study identified a gradient of connectivity across the structure with respect to connectivity with ventral striatum and midbrain ([Kahn and Shohamy, 2013](#)). While resting fMRI methods infer differential functional connectivity by comparing BOLD variations across time in a single brain state, such networks have the drawback that they lack a functional or neuropsychological context. Resting fMRI studies also tend to focus on particular frequency bands and stationary association, an approach which has proved highly robust but may only reflect a limited range of inter-regional information transmission.

Further characterization of functional connectivity may be obtained by alternative approaches, including meta-analytic connectivity modeling (MACM). In the MACM approach, the inference of functional interactions is based on the co-occurrence of significant activations across studies. While in practice, networks identified by MACM appear to correspond well to those identified by direct covariance using fMRI, discrepancies have also been noted (cf. [Clos et al., 2013](#); [Eickhoff et al., 2014](#); [Jakobs et al., 2012](#)). In general, a good corroboration of MACM-based or similar approaches with well-established brain functional connectivity patterns is seen ([Clos et al., 2014](#); [Crossley et al., 2013](#); [Di et al., 2013](#)). Nevertheless, distinct properties of MACM-estimated functional connectivity on large scale connectivity networks have been identified, which may reflect, at first approximation, the influence of a general task set ([Crossley et al., 2013](#); [Di et al., 2013](#)). Neurofunctional context may be particularly relevant for understanding the functional connectivity of the hippocampal formation, as information transmission to and from the region can be modulated both by behavioral context and input from a third region (e.g. [Belujon and Grace, 2008](#); [Gill and Grace, 2013](#)). A recent development for functional mapping has been to examine patterns of differential connections via clustering algorithms to demonstrate distinct subregions with internally coherent connectivity within large anatomical structures ('connectivity-based parcellation'). In particular, data driven clustering based on MACM maps has been employed to demonstrate distinct subregions of the amygdala ([Bzdok et al., 2012](#)), supplementary motor area ([Eickhoff et al., 2011](#)), temporo-parietal junction ([Bzdok et al., 2013](#)) and dorso-lateral prefrontal cortex ([Cieslik et al., 2013](#)).

To our knowledge, a data-driven parcellation of the hippocampal formation using MACM maps has not been conducted (but see [Bonnici et al., 2012](#)). However, given the complexity of the hippocampal formation, with respect to its geometry, anatomical differentiation and connectivity, we focused on the subiculum rather than the entire region. Continuous with the CA1 region of the hippocampus, but located within the parahippocampal gyrus in humans ([Duvernoy, 2005](#)), the subiculum provides a central role in the integration of information within the hippocampus ([Naber et al., 2000](#)) as well as its transmission to

other brain regions ([Witter, 2006](#)). The subiculum has also gained attention in the context of pathophysiological models for a variety of psychiatric conditions, in particular those with a component reflecting maladaptive responses to stress ([Herman and Mueller, 2006](#)), including schizophrenia, addiction and mood disorders ([Belujon and Grace, 2014](#); [Grace, 2010](#)). Consistent with the presence of functional differentiation across the structure, distinct behavioral consequences of dorsal and ventral subiculum manipulations have been observed in rodents ([Andrzejewski et al., 2006](#); [Caine et al., 2001](#)). The dorsal-most regions of the subiculum are known to contain place cells which encode location within the spatial domain ([O'Mara, 2006](#)). However, as one moves ventrally, this location information is overlaid with limbic inputs. Thus, ventral regions are able to encode the emotional salience of a location, consistent with a contextual signal ([Grace, 2012](#)). This functional segregation is mirrored by distinct patterns of anatomical connectivity across the rodent subiculum. The entire structure is connected to the septum, thalamus, mammillary bodies and retrosplenial cortex, although each region receives topographically organized projections. In addition, the ventral subiculum is connected to orbital and medial prefrontal cortex, nucleus accumbens ([Aggleton, 2012](#); [Groenewegen et al., 1987](#); [Witter, 2006](#)), and shows bidirectional connectivity with the amygdala ([French et al., 2003](#)). Anterior cingulate and prelimbic regions of the rodent prefrontal cortex receive input from the dorsal subiculum, whereas infralimbic regions receive input from ventral subiculum ([Witter, 2006](#)). Finally, some investigations have hinted at the presence of an intermediate region with mixed anatomical connectivity ([Groenewegen et al., 1987](#); [Strange et al., 2014](#); [Wright et al., 2013](#)).

Although the small size of the subregion and the resolution of imaging studies within the BrainMap database provides an upper limit on our ability to distinguish the subiculum per se from other nearby regions, this region was chosen as a seed for our analyses for two principle reasons: first, as the subiculum is generally considered to be an important output node through which the hippocampus proper communicates with downstream regions, estimates of functional connectivity are likely to be interpretable in terms of the pattern of known efferent connections from the region. Moreover, a prevailing interpretation of local BOLD signals (e.g. [Bartels et al., 2008](#)) might suggest that regions which receive synaptic input directly from the hippocampus should provide a promising place for initial focus. Second, the region, as defined by the cytoarchitectonic work of [Amunts et al. \(2005\)](#) is a relatively long, thin structure which traverses the entire anterior/posterior axis of the hippocampal formation. Although this limited resolution in the medial-lateral dimension, it provided a potential for discrimination in the dimension of interest. We were therefore optimistic that a data-driven parcellation of the region would reflect the functional differentiation across the anterior/posterior axis of the hippocampal formation.

In the present study, we aimed to map the subiculum based on regional patterns of functional connectivity using whole brain maps describing the co-occurrence of significant activations across studies. These maps were generated using the BrainMap database for each voxel within the subiculum. The cross-correlation of whole-brain co-occurrence of significant activations between each pair of seed voxels within the subiculum was computed. Clusters of seed voxels with similar patterns of connectivity were determined. The obtained clusters were cross-validated using multivariate clustering methods ([Clos et al., 2013](#)). We also aimed to map the (specific) whole-brain interaction pattern of the identified subregions using both task (using MACM) and resting state (examining variation in low frequency resting state BOLD) functional connectivity analyses. We investigated the extent to which the MACM and resting fMRI signals overlapped by using activation loci defined by the former to mask the latter, as well as performing whole brain analyses of each. A final aim was to characterize the functions of the resulting sub-regions with reference to the behavioral taxonomy information in the BrainMap database. We performed a functional characterization of the region via statistical forward and reverse

inference, aiming to understand more precisely the region's role in mnemonic (Carr et al., 2013), spatial (Suthana et al., 2011), motivational (Andrzejewski et al., 2006) and other cognitive processes.

Specific hypotheses regarding connectivity were tested with reference to aforementioned models of the hippocampal formation which emphasize long-axis functional differentiation (e.g. Strange et al., 2006; Caine et al., 2001; Lodge and Grace, 2008, 2011; Valenti et al., 2011). In addition, the subiculum has a bidirectional relationship with the basolateral amygdala (French et al., 2003) which may modulate the interaction with the ventral striatum (Gill and Grace, 2011, 2013). Consequently, we anticipated that the anterior subiculum would show strong connectivity with the amygdala and ventral striatum. We also anticipated that the subiculum would be functionally connected to regions within the default mode network (DMN), given that the hippocampal formation is considered part of the DMN (Andrews-Hanna et al., 2010b; Lu et al., 2012), and regions such as the retrosplenial cortex and nearby posterior cingulate cortex show consistent patterns of anatomical connectivity across the whole subiculum (Aggleton et al., 2012). It is important to emphasize that, due to the interconnectivity of different hippocampal subregions and the level of effective resolution afforded by the BrainMap database, the obtained parcellation structure is likely to reflect the organizational structure of the hippocampal formation as a whole, rather than reflecting the subiculum per se. In this light, a subsequent parcellation was performed on a Cornu Ammonis/Dentate Gyrus region of interest (Amunts et al., 2005).

Methods

Definition of the region of interest

The volume of interest (VOI) that formed the basis of our investigation was derived from a histological definition of the subiculum using the SPM Anatomy Toolbox (Eickhoff et al., 2005). The bilateral subiculum, along with adjacent medial temporal lobe (MTL) structures, have previously been cytoarchitecturally mapped in 10 human post-mortem brains, 3D reconstructed, and registered to MNI (Montreal Neurological Institute) reference space (Amunts et al., 2005). The overlap of these as well as histological information on the surrounding structures were used to generate a "maximum probability map" (MPM) of the hippocampal formation. This MPM reflects the most likely cortical fields at each brain voxel, and provides a discrete representation of microanatomically defined brain areas in standard space. The seed region for the current analysis was thus defined by the MPM representation of the human subiculum (Amunts et al., 2005), a VOI defined to include voxels where the subiculum had been more likely to be found than any other MTL structure in histological examination of the 10 individuals. A follow up analysis was conducted using a combined Cornu Ammonis/Dentate Gyrus region of interest, which had also been defined using the same method (Amunts et al., 2005).

Meta-analytic connectivity mapping (MACM)

The co-occurrence of significant activations across studies within each voxel within the subiculum VOI were computed, using data from the BrainMap database (www.brainmap.org; Fox and Lancaster, 2002; Laird et al., 2011). From this database, studies reporting fMRI and PET experiments in stereotaxic space from "normal mapping" studies in healthy participants, without interventions or group comparisons, were included. Approximately 7200 functional neuroimaging experiments that satisfied these criteria were considered for the current analysis. The co-ordinates from these maps are all registered within MNI space. The MACM analysis is based on the identification of all of the BrainMap experiments where a given seed voxel is activated. However,

often the voxelwise activation is too sparse for subsequent integration of activation loci. To increase the reliability of connectivity estimates, BrainMap experiments were pooled which reported activation in the vicinity of each seed voxel. The width of the spatial filter used to identify the experiments was systematically varied by including the 20 to 200 experiments which are closest to a given seed voxel in steps of five (i.e. 20, 25, 30, 35, ..., 200 experiments). Proximity was assessed by calculating the Euclidian distances between a given seed voxel and any activation reported in BrainMap, and sorting the experiments on this basis. Next, the n-nearest activation foci were selected, where n is the size of the spatial filter. As expected, this procedure successfully provided activation foci proximal to seed voxel. Specifically, the average distance between the seed voxel and activation foci included for that voxel varied from 4.09 mm (i.e. ~2 voxels) when the closest 20 experiments were included to 8.72 mm (i.e. ~4 voxels) when 200 experiments were included. The standard deviation across voxels likewise increased with increasing filter size from 0.720 mm (20 experiments) to 0.9 mm (200 experiments).

Subsequently, a coordinate-based meta-analysis was performed on the retrieved experiments, generating a brain-wide co-occurrence of activation profile of a given seed voxel, for each of the 37 filter sizes. The brain-wide pattern of co-occurrence for each individual seed voxel was computed by activation likelihood estimation (ALE: Eickhoff et al., 2012; Eickhoff et al., 2009; Turkeltaub et al., 2002) meta-analysis over the experiments that were associated with that particular voxel by the pooling procedure outlined above. The key idea behind ALE is to treat the foci reported in the associated experiments not as single points, but as centers for 3D Gaussian probability distributions that reflect the spatial uncertainty associated with neuroimaging results. For each experiment, the probability distributions of all reported foci were then combined into a modeled activation (MA) map for that particular experiment (Turkeltaub et al., 2012). The voxel-wise union of these values (across all experiments associated with a particular seed voxel) then yielded an ALE score for each voxel of the brain that describes the co-occurrence probability of each particular location in the brain with the current seed voxel. The ALE scores of all voxels within the gray matter (based on 10% probability according to the ICBM (International Consortium on Brain Mapping) tissue probability maps) were then recorded before moving to the next voxel of the seed region. In contrast to conventional applications of ALE, no thresholding was performed at this stage as no inference was sought. Instead, we aimed to create a whole-brain map of co-occurrence probabilities for each seed voxel, and use this profile as a basis for parcellation of the VOI. The highest convergence is evidently found at the location of the seed, as experiments are pooled on the basis of their proximity to the seed. However, significant convergence at more distal locations is evidence of reproducible co-occurrence of activations across experiments.

Connectivity-based parcellation

The unthresholded brain-wide co-occurrence profiles for all seed voxels were then combined into a $NS \times NT$ co-occurrence matrix, where NS denotes the number of seed voxels in the subiculum (1509 voxels at $2 \times 2 \times 2 \text{ mm}^3$ resolution) and NT the number of target voxels in the reference brain volume at $2 \times 2 \times 2 \text{ mm}^3$ resolution (approximately 30,000 gray matter voxels at a resolution of $4 \times 4 \times 4 \text{ mm}^3$). $4 \times 4 \times 4 \text{ mm}^3$ was the resolution used for the co-occurrence map (NT) dimension, to reduce matrix redundancy and for computational expediency. K-means clustering (Matlab, Mathworks, USA) was used to parcellate the subiculum VOI with $K = 2, 3, \dots, 9$. K-means clustering is a non-hierarchical clustering method that uses an iterative algorithm to separate the seed region into a previously selected number of K non-overlapping clusters (Hartigan and Wong, 1979). K-means aims at minimizing the variance within clusters and maximizing the variance between clusters by first computing the centroid of each cluster and subsequently reassigning voxels to the clusters such that

327 their difference from the centroid is minimal. The distance measure
 328 used was one minus the correlation between the co-occurrence pat-
 329 terns of seed voxels defined above (correlation distance). Importantly,
 330 maps of co-occurrence of activations were computed for each of the
 331 37 different spatial filter sizes (see above), and the K-means parcellation
 332 was performed for each filter size independently, yielding 8 (K number
 333 of clusters) \times 37 (filter size) independent cluster solutions (Clos et al.,
 334 2013). To avoid local minima, optimal solutions were determined
 335 from 25 replications of each parcellation, using random initial condi-
 336 tions (centroids).

337 Selection of optimal filter range

338 Following previous work on the inferior frontal gyrus (Clos et al.,
 339 2013), our approach to selecting the optimal solution of K-means clus-
 340 tering from the 8 (K clusters) by 37 (filter sizes) solutions was to exam-
 341 ine the properties of these various solutions and establish the most
 342 stable range of filter sizes. This prevented a combinatorial expansion
 343 of possible solutions, and avoided the requirement of averaging across
 344 filter sizes (Bzdok et al., 2012; Cieslik et al., 2013). We implemented
 345 a two-step procedure that involved a decision on those filter-sizes
 346 (from the broad range of processed ones) to be included in the final
 347 analysis and subsequently a decision on the optimal cluster-solution.
 348 In the first step, we examined the consistency of the cluster assign-
 349 ment for the individual voxels across the cluster solutions of the co-
 350 occurrence maps performed at different filter sizes. We selected a filter
 351 range with the lowest number of deviants, i.e., number of voxels that
 352 were assigned differently compared with the solution from the majority
 353 of filters. In other words, we identified those filter sizes which produced
 354 solutions most similar to the consensus-solution across all filter sizes.
 355 The proportion of deviants (normalized within each cluster-solution
 356 K), illustrated in Supplemental Fig. 2, indicates that most deviants
 357 were present in parcellations based on small filter sizes. As previously
 358 described (Clos et al., 2013), we chose the borders of the filter range
 359 (85 to 200) based on the z-scores of the number of deviants (Supple-
 360 mental Fig. 2), and this restricted range was used in all subsequent
 361 steps.

362 Selection of the optimal number of clusters

363 The second step was to determine the optimal solution of K within
 364 the restricted filter range of filter sizes. We considered three criteria
 365 representing the characteristics of the cluster solutions, reflecting topo-
 366 logical, information-theoretic and cluster separation properties (see
 367 Supplemental Fig. 2). First, misclassified voxels (deviants) represent
 368 an important topological criterion, as they indirectly reflect the amount
 369 of noise and local variance. We thus employed a criterion which
 370 addressed the across-filter stability: using the most frequent (mode)
 371 assignment of these voxels across all filter sizes as a reference point,
 372 the percentage of deviants for each filter-size that were assigned to a
 373 different cluster were computed. Optimal K parcellations were those
 374 where the percentage of deviants was not significantly increased
 375 compared to the K-1 solution, and in particular, those where the subse-
 376 quent K + 1 solution also lead to a significantly higher percentage of
 377 deviants.

378 Second, the similarity of cluster assignments for each filter size be-
 379 tween the current solution and the neighboring (K-1 and K + 1) solu-
 380 tions was employed as an information theoretic criterion. We used the
 381 variation of information (VI) metric (Meila, 2007), which has also
 382 been employed in previous neuroimaging studies (Kahnt et al., 2012).
 383 For each filter size the VI metric was computed between a given K solu-
 384 tion and the subsequent K + 1 solution. Solutions were considered sta-
 385 ble if there was a significant increase in VI between the subsequent set
 386 of solutions (primary criterion) or if there was a significant decrease
 387 from the previous to the current clustering step (secondary criterion).

Third, as a cluster separation criterion, the silhouette value averaged
 across voxels for each filter size was considered. The silhouette value is a
 measure of how similar that voxel is to voxels in its own cluster com-
 pared to voxels in other clusters, and ranges from -1 to $+1$. Good so-
 lutions are those with a significantly higher silhouette value compared
 to the K-1 solution (primary criterion) or whose silhouette value is at
 least not significantly decreased compared to the previous K-1 solution
 (secondary criterion).

Visualization of the best cluster solution

A five cluster solution was identified as the most stable parcellation
 (see Supplemental Fig. 1). Only voxels located in the gray matter and
 hierarchically and spatially consistent were considered for subsequent
 analyses, resulting in 1373 out of the originally 1509 subiculum voxels
 in the identified subregions. Multidimensional scaling (MDS) was
 used to visualize the 2-dimensional cluster separation. We computed
 the NS \times NS correlation distance matrix (see [Connectivity-based
 parcellation](#) section) for each of the 24 filter sizes. Next, MDS was per-
 formed on the eigenimage of the 24 correlation distance matrixes.
 Sammon's nonlinear mapping was used as the goodness-of-fit criterion.
 Finally, the locations of the five clusters were mapped back on the brain,
 taking the mode across filter sizes. The resulting clusters were individu-
 ally median-filtered to create smooth, continuous structures. These fil-
 tered subregions were used for subsequent functional connectivity
 and BrainMap analyses.

Task-dependent connectivity: co-occurrence of significant activations across studies

The functional connectivity of the subregions was first assessed
 using meta-analytic connectivity modeling (MACM). For this, all exper-
 iments in the BrainMap database that featured at least one focus of acti-
 vation in a particular subregion were compiled. In contrast to the MACM
 underlying the co-occurrence based parcellation, where ALE maps were
 not thresholded to retain the complete pattern of likelihoods of co-
 occurrence, statistical inference was now performed. Inference was per-
 formed with reference to a null-distribution reflecting a random spatial
 association between experiments with a fixed within-experiment dis-
 tribution of foci (Eickhoff et al., 2009). This random-effects inference as-
 sesses above-chance convergence between experiments, not clustering
 of foci within a particular experiment. The observed ALE scores from the
 actual meta-analysis of experiments activating within a particular clus-
 ter were then tested against the ALE scores obtained under a null-
 distribution reflecting random spatial association, yielding a p-value
 based on the proportion of equal or higher random values (Eickhoff
 et al., 2012). The resulting non-parametric p-values were transformed
 into Z-scores and thresholded at a cluster-level Family Wise Error
 (FWE) rate-corrected threshold of $p < 0.05$ (cluster-forming threshold
 at voxel-level $p < 0.001$).

We computed the overlap between the brain-wide co-occurrence
 patterns of the five connectivity-derived clusters using a minimum-
 statistic conjunction, i.e., by computing the intersection of the thresh-
 olded ALE-maps (Caspers et al., 2010). Next, we tested for differences
 in co-occurrence patterns between all pairs of clusters by performing
 MACM separately on the experiments associated with either cluster
 and computing the voxel-wise difference between the ensuing ALE
 maps. All experiments contributing to either analysis were then pooled
 and randomly divided into two groups of the same size as the two orig-
 inal sets of experiments defined by activation in the first or second clus-
 ter (Eickhoff et al., 2011). ALE-scores for these two randomly assembled
 groups were calculated and the difference between these ALE-scores
 was recorded for each voxel in the brain. Repeating this process
 10,000 times then yielded a null-distribution of differences in ALE-
 scores between the MACM analyses of the two clusters. The 'true' differ-
 ence in ALE scores was then tested against this null-distribution yielding

450 a posterior probability that the true difference was not due to random
451 noise in an exchangeable set of labels based on the proportion of
452 lower differences in the random exchange. The resulting probability
453 values were then thresholded at $p > 0.95$ (95% chance for true differ-
454 ence) and inclusively masked by the respective main effects, i.e., the sig-
455 nificant effects in the MACM for the particular cluster.

456 In addition, we examined the MACM maps of the clusters at each
457 level of parcellation, up to the most stable 5 cluster solution. We always
458 compared the newly emerged child cluster with its remaining parent
459 cluster at the same level of K . Thus, we report the MACM analyses asso-
460 ciated with cluster 1 vs. 2 at the level of $K = 2$, cluster 3 vs. 2 at $K = 3$,
461 cluster 4 vs. 1 at $K = 4$, and cluster 5 vs. 3 at $K = 5$.

462 Task-independent connectivity: “resting state”

463 In addition, we also delineated the task independent resting-state
464 functional connectivity pattern of each cluster. Resting state fMRI
465 images of 153 healthy volunteers (mean age 41.1 ± 18.0 years; 92
466 males) from the NKI/Rockland sample were obtained through the
467 1000 Functional Connectomes Project (www.nitrc.org/projects/fcon_1000/). During the resting state scans subjects were instructed to keep
468 their eyes closed and to think about nothing in particular but not to
469 fall asleep (which was confirmed by post-scan debriefing). For each
470 subject 260 resting state EPI images were acquired on a Siemens
471 TimTrio 3T scanner using blood-oxygen-level-dependent (BOLD) con-
472 trast (gradient-echo EPI pulse sequence, TR = 2.5 s, TE = 30 ms, flip
473 angle = 80° , in plane resolution = 3.0×3.0 mm², 38 axial slices
474 (3.0 mm thickness) covering the entire brain). The first four scans
475 were excluded from further processing analysis using SPM8 to allow
476 for magnet saturation. The remaining EPI images were first corrected
477 for movement artifacts by affine registration using a two pass pro-
478 cedure in which the images were first aligned to the initial volumes
479 and subsequently to the mean after the first pass. The obtained mean
480 EPI of each subject was then spatially normalized to the MNI single sub-
481 ject template using the ‘unified segmentation’ approach (Ashburner
482 and Friston, 2005). The ensuing deformation was applied to the individ-
483 ual EPI volumes. To improve signal-to-noise ratio and compensate for
484 residual anatomical variations images were smoothed with a 5-mm
485 Full Width Half Maximum (FWHM) Gaussian kernel.

486 In line with conventional methods of rsfMRI analysis, the time-series
487 data of each voxel were corrected for the following nuisance variables
488 (cf. Jakobs et al., 2012; Satterthwaite et al., 2012): the six motion param-
489 eters derived from the realignment step, and their first derivative;
490 timeseries reflecting mean gray matter, white matter and cerebrospinal
491 fluid, obtained by averaging across voxels assigned to the respective tis-
492 sue classes by the SPM8 segmentation step. After regressing out these
493 variables, the resulting residual timeseries were band pass filtered be-
494 tween 0.01 and 0.08 Hz, as the majority of the power of the rsfMRI
495 BOLD signal is present at these frequencies (Baria et al., 2013).

496 We used the five CBP-derived clusters as seeds for the resting state
497 analysis. Linear (Pearson) correlation coefficients between the time
498 series of the seed regions and all other gray matter voxels in the brain
499 were computed to quantify rsfMRI connectivity. These voxel-wise
500 correlation coefficients were then transformed into Fisher’s Z-scores
501 and tested for consistency in a flexible factorial model across subjects.
502 The main effect of connectivity for each cluster as well as planned con-
503 trasts between the clusters were tested using the standard SPM8
504 implementations with the appropriate non-sphericity correction.
505 These analyses were thresholded at $p < 0.05$ (FWE cluster-corrected;
506 cluster-forming threshold at voxel-level $p < 0.001$). A second analysis
507 was performed to investigate the similarity between the MACM and
508 resting state analyses: rsfMRI Z-score maps were masked using the
509 thresholded maps from the MACM analysis: inference was performed
510 only within the regions identified as co-activated by a MACM analysis
511 using the corresponding subregion as a seed. A cluster was reported
512 as significant in Table 2 if a FWE-corrected voxelwise threshold of
513

$p < 0.05$ was reached (corrected for voxels within the MACM mask rath-
514 er than the whole brain). 515

Functional characterization: meta-data 516

517 The functional characterization of the CBP-derived clusters was
518 based on the ‘Behavioral Domain’ and ‘Paradigm Class’ meta-data cate-
519 gories available for each neuroimaging experiment included in the
520 BrainMap database. Behavioral domains include the main categories
521 cognition, action, perception, emotion, and interoception, as well as
522 their related sub-categories. Paradigm classes categorize the specific
523 task employed (see <http://brainmap.org/scribe/> for the complete
524 BrainMap taxonomy).

525 In a first step, we determined the individual functional profile of
526 the five CBP derived clusters by using forward and reverse inference
527 (Bzdok et al., 2013; Cieslik et al., 2013; Rottschy et al., 2013). Forward
528 inference is the probability of observing activity in a brain region
529 given knowledge of the psychological process, whereas reverse infer-
530 ence is the probability of a psychological process being present given
531 knowledge of activation in a particular brain region. In the forward in-
532 ference approach, a cluster’s functional profile was determined by iden-
533 tifying taxonomic labels, for which the probability of finding activation
534 in the respective cluster was significantly higher than the overall chance
535 (across the entire database) of finding activation in that particular clus-
536 ter. Significance was established using a binomial test ($p < .05$, corrected
537 for multiple comparisons with reference to the False Discovery Rate
538 (FDR)). Thus we tested whether the conditional probability of activation
539 given a particular label ($P(\text{Activation}|\text{Task})$) was higher than the base
540 rate probability of activating a given subregion per se ($P(\text{Activation})$).
541 In the reverse inference approach, a cluster’s functional profile was de-
542 termined by identifying the most likely behavioral domains and para-
543 digm classes given activation in a particular subregion. This likelihood
544 $P(\text{Task}|\text{Activation})$ can be derived from $P(\text{Activation}|\text{Task})$ as well as
545 $P(\text{Task})$ and $P(\text{Activation})$ using Bayes’ rule. Significance was then
546 assessed by means of a chi-square test ($p < .05$, FDR corrected).

Results 547

Subicular parcellation based on co-occurrence of significant activations 548 across studies 549

550 As already noted in the methods, our identification of the optimal
551 level for the K-means clustering of the subiculum VOI yielded a best so-
552 lution at $k = 5$ (Fig. 1). This solution indicated a bilateral anterior region,
553 and distinct left and right posterior and intermediate regions (Fig. 2).
554 Notably, there was no a priori bias toward the identification of bilateral
555 or unilateral regions in this analysis, and indeed running the same algo-
556 rithm with unilateral subiculum regions yielded a similar pattern of
557 three clusters per hemisphere. The derived clusters were of similar
558 sizes, and there was no obvious asymmetry in the location of the poste-
559 rior and intermediate subregions across the hemispheres.

560 Although some voxels from outside of the subiculum ROI (e.g. ento-
561 rhinal cortex) were included in the initial parcellation, these represent-
562 ed a tiny minority of each cluster, and were caused by downsampling
563 the subiculum mask for the cluster analysis. Moreover, these were
564 mostly removed by the filtering, leaving final clusters that were almost
565 entirely restricted to the subiculum ROI alone. Only the anterior subre-
566 gion (left hemisphere 96.2% and right hemisphere 99.3% of voxels with-
567 in ROI) and the right intermediate subregion (98.2% within) had any
568 voxels outside of the original subiculum ROI.

569 To test the specificity of this parcellation to the subiculum, we per-
570 formed a follow-up analysis of a combined Cornu Ammonis/Dentate
571 Gyrus (CA/DG) region of interest using the same methodological
572 approach. A very similar pattern of parcellation provided the best fit,
573 including a single bilateral anterior region, and separate left- and
574 right-focused intermediate and posterior regions (see Fig. 3). A slight

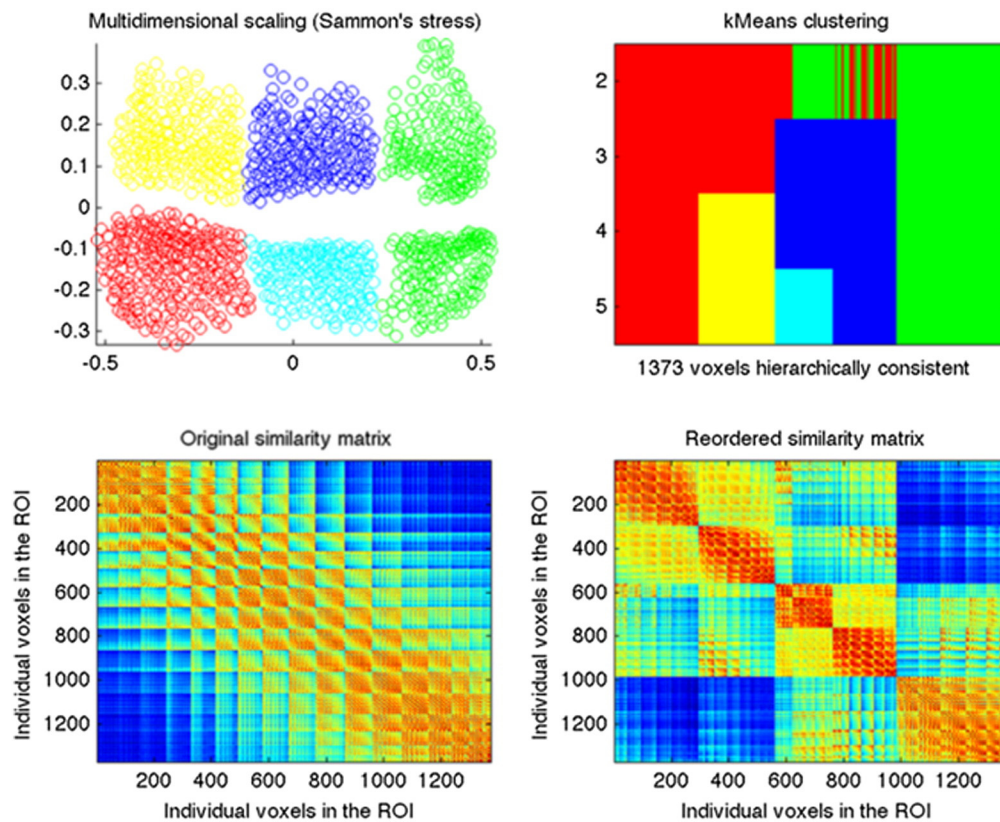


Fig. 1. Visualization of properties of the best cluster solution ($K = 5$). Color coding: green = bilateral anterior; cyan = right intermediate; blue = left intermediate; red = right posterior; yellow = left posterior. Top left: visualization of the 5-cluster solution by multidimensional scaling. Points (voxels) which are closer together have more similar co-occurrence maps. Top right: cluster assignment and splitting of clusters across levels of K . Bottom left: similarity matrix of the seed voxels in the original data. Bottom right: similarity matrix of the seed voxels reordered in terms of the K -means clustering parcellation.

Data obtained from BrainMap database.

575 difference was that the right posterior subregion was coupled with a
576 smaller cluster on the left hand side (i.e. was partially bilateral).
577 Parcellation fit metrics are included in the supplementary information
578 (Supplemental Fig. 3).

579 MACM analyses of subicular subregions

580 Individual MACM analyses for each subregion revealed that, in spite
581 of several common aspects, the main effect of each subregion was also
582 associated with distinct patterns of co-occurrence of significant activa-
583 tions across studies (Table 1; Fig. 4). The anterior cluster was associated
584 with a cluster within the ventromedial prefrontal cortex (vmPFC). The
585 intermediate and posterior subregions were more similar and generally
586 associated with activation in a dorsomedial frontal location, at the nexus
587 between dorsal and mid ACC and the supplementary motor area (SMA).
588 Co-occurrence of activations was also observed in the left lateral pre-
589 frontal cortex, although the distribution of resulting clusters differed be-
590 tween the seed subregions. The intermediate and posterior subregions
591 were also commonly associated with discrete activations in posterior
592 regions such as the fusiform and calcarine gyri. The right posterior
593 subicular subregion showed a unique pattern of activation in the bilat-
594 eral putamen and anterior insula. Both posterior subregions showed
595 thalamic activation. Direct comparison of the MACM connectivity
596 maps largely revealed significant differences in regional connectivity
597 in the regions identified by the initial subregion analysis (Table 1): so
598 if a region was identified as being co-activated with a particular
599 subiculum subregion, this region would usually show greater activation
600 than any of the other subiculum subregions, at least within part of the
601 co-occurrence cluster. In parallel with this finding, conjunction analyses
602 revealed only minor convergent activations outside of the hippocampal

603 complex: conjunctions across two subregions were restricted to co-
604 occurrence within some intermediate and posterior regions within the
605 SMA (Table 1).

606 Examination of the MACM connectivity associated with sub-optimal
607 cluster solutions lower than 5 suggested that the initial separation of
608 clusters was in terms of an anterior vs. middle/posterior divide (Supple-
609 mental Fig. 4). At the point of the first separation, the anterior cluster
610 was uniquely identified by its association with two DMN structures,
611 a region of ventromedial PFC and posterior cingulate cortex (PCC),
612 while the posterior region was better associated cortical structures
613 with subcortical structures (lateral putamen, thalamus) and posterior
614 cortical activation. However, both subregions were co-activated with
615 supplementary motor area and left lateral PFC. These latter structures
616 were the point of divergence at the next separation, with an anterior
617 region co-activated with the vmPFC (but no longer PCC) separating
618 from an intermediate region co-activated with SMA and left lateral
619 PFC. The next split was between left and right posterior subiculum,
620 where the right posterior region remained associated with the putamen
621 and anterior insula, whereas the left posterior region was associated
622 with a large co-occurrence cluster in left lateral prefrontal cortex and
623 a distinct cluster in left occipital cortex. The final split was between
624 left and right intermediate subregions: again, the left hemisphere region
625 was associated with a substantial left lateral prefrontal cluster, whereas
626 the right was distinguished by cluster in the right fusiform gyrus.

627 Functional connectivity of subicular subregions using rsfMRI

628 In order to complement the above findings, we also examined the
629 resting-state functional connectivity of each of the five subregions,
630 again using each as seed regions. First, we examined the positive and

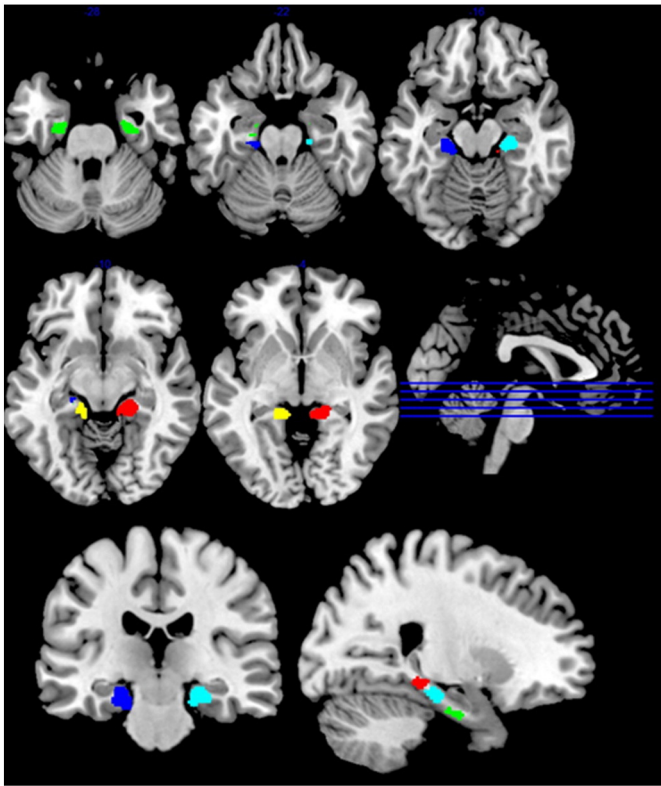


Fig. 2. Initial parcellation of subiculum (green = bilateral anterior; cyan = right intermediate; blue = left intermediate; red = right posterior; yellow = left posterior). Data obtained from BrainMap database.

631 negative correlations with each region, masked by the MACM findings
 632 for the respective subregion (Table 1: SVC voxel wise corrected
 633 $p < 0.05$). These analyses showed that, in general, regions identified
 634 by the MACM analysis also showed voxels with positive resting correlations
 635 with the corresponding subiculum subregion. There were a
 636 few exceptions: most importantly that regions of the SMA and left
 637 PFC, previously identified by the MACM analysis to be co-activated
 638 with intermediate and posterior regions, showed *negative* associations

(anti-correlation) with resting bold in the corresponding subiculum
 639 subregion. 640

We also examined the unmasked main effects (Supplemental
 641 Table 1: Fig. 5) and systematically performed planned comparisons
 642 between the five subregions (Supplemental Table 2; Fig. 6) across the
 643 whole brain (FWE clusterwise correction $p < 0.05$). Individual analysis
 644 of each seed region revealed that, in general, all subregions were
 645 functionally connected with the medial PFC, PCC/retrosplenial cortex,
 646 precuneus, as well as the inferior parietal/angular gyrus (PGp) and anterior
 647 temporal regions in anterior and intermediate subregions. Likewise,
 648 all subregions were negatively coupled with 'task positive' regions such
 649 as the dorsolateral and inferior PFC, superior parietal lobule (SPL 7A),
 650 inferior parietal cortex (PF/PFm; HIP3), dorsal ACC/SMA, anterior insula or
 651 visual regions (Supplemental Table 1). Taken together, the whole brain
 652 and MACM-masked analyses gave contrasting pictures of subiculum
 653 functional connectivity. Put simply, aside from the anterior subiculum,
 654 regions such as the PCC or medial PFC which were strongly functionally
 655 coupled to the subiculum in the rsfMRI analysis were not identified in
 656 the MACM analysis. Moreover, regions identified in the MACM analysis –
 657 the left lateral PFC and SMA – were negatively coupled with the
 658 subiculum in the rsfMRI analysis. Thus, regions outside the hippocampus
 659 which showed *both* MACM clusters and rsfMRI positive connectivity
 660 were present but somewhat sparse: the anterior subiculum seed
 661 showed such a conjunction in the vmPFC; bilateral posterior seeds
 662 co-activated in discrete sectors of the occipital cortex; left intermediate
 663 seed showed a conjunction in the retrosplenial/precuneus; and right
 664 posterior seed showed a conjunction in the right insula. 665

We also performed pairwise contrasts between anterior, bilateral
 666 intermediate (left and right combined) and bilateral posterior seeds
 667 (Supplemental Table 2, Fig. 6). We observed that anterior regions
 668 were more strongly functionally connected to several regions of medial
 669 PFC – extending through the orbitofrontal cortex, rostromedial PFC and
 670 dorsomedial PFC (although generally not including the ventral ACC), as
 671 well as the PCC and inferior parietal/angular gyrus, while intermediate
 672 and posterior regions were better associated with regions such as the
 673 dorsal ACC/SMA, anterior insula, bilateral dorsolateral PFC, dorsal striatum,
 674 medial thalamus, the fusiform gyrus and inferior (PF) and superior
 675 parietal (SPL). 676

In addition to identifying a relationship between the subiculum and
 677 cortical brain networks, the subiculum was functionally connected with
 678 specific subcortical regions, broadly consistent with our hypotheses
 679

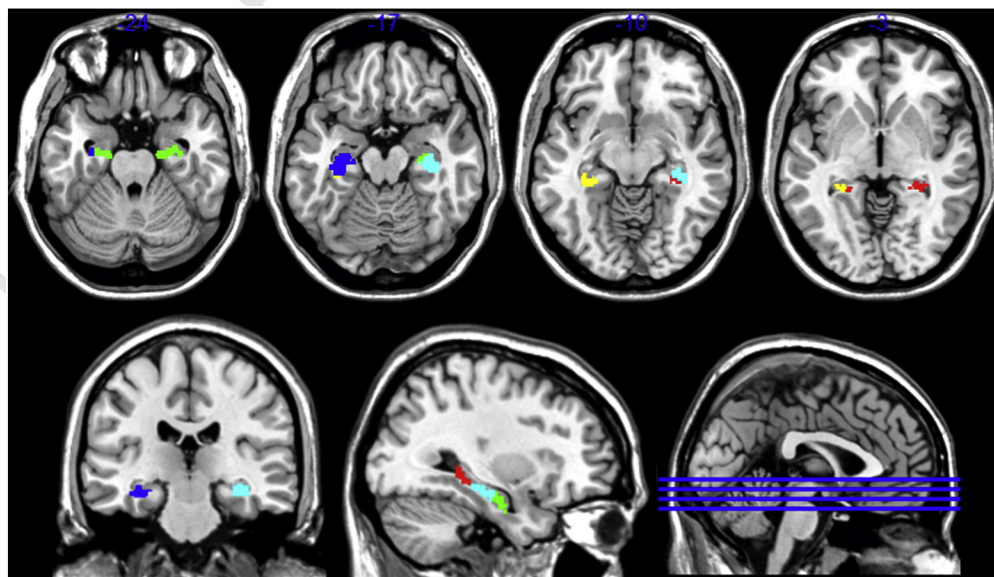


Fig. 3. Parcellation of CA/DG region of interest (green = bilateral anterior; cyan = right intermediate; blue = left intermediate; red = right posterior; yellow = left posterior). Data obtained from BrainMap database.

Table 1

Table denoting regions associated with MACM analysis, for each subregion (whole brain FWE corrected threshold). "Resting fMRI correlation" denotes the presence of a significant (small volume corrected) positive or negative correlation of low frequency BOLD of the corresponding subiculum subregion in a given MACM cluster ('convergent connectivity'). Cluster size, provided in parentheses, is determined using a cluster forming threshold of $p < 0.001$ uncorrected. "MACM contrast" denotes the presence of a significant difference in the modeled activation scores, in terms of contrasts (>: modeled activation in region A is greater than B) and conjunctions (=: regions A and B both coactivate the cluster) of different subregions (minimum cluster size reported 15 voxels). Ant = anterior; LI = left intermediate; RI = right intermediate; LP = left posterior; RP = right posterior.

Cluster 1 (right posterior)	Peak voxel (X Y Z)	Size (voxels)	rsfMRI correlation	MACM contrast (voxels)
Left hippocampus (SUB)	− 18 − 32 − 8	1730	Positive (1047)	> Ant (subiculum/thalamus 868; pallidum/insula 348)
Left amygdala (SF)				= Ant (392)
Left thalamus (parietal)				> LI (subiculum/thalamus 340; insula 206; pallidum 68)
Left pallidum				= LI (655)
Left anterior insula				> LP (insula 127; amygdala 63)
Right hippocampus (SUB/CA)	18 − 32 − 8	1128	Positive (1069)	> RI (subiculum/thalamus 423; pallidum 79)
Right thalamus (parietal/temporal)				> Ant (1028)
				> LI (869)
				= LI (491)
				> LP (953)
				> RI (862)
Supplementary motor area, MCC	− 2 20 48	500	Negative (137)	> Ant (422)
				> LI (53)
				= LI (237)
				> LP (38)
				> RI (229)
Left fusiform gyrus	− 42 − 62 − 20	406	Positive (68)	> Ant (343)
Left cerebellum (lobules V, VI, VIIa)				> LI (fusiform/VIIa 319; VI 78)
				> LP (VI 68; VIIa 40)
				> RI (VI/VII 189; V/VI 103)
Right anterior insula, inferior frontal gyrus	42 20 − 6	363	Positive (43)	> Ant (304)
				> LI (128)
				> LP (189)
				> RI (202)
Lingual, calcarine gyrus	4 − 70 2	335	Positive (58)	> Ant (259)
				> LI (208)
				> LP (144)
				> RI (152; 39)
Right pallidum, putamen	16 2 2	199	None	> Ant (192)
				> LI (126)
				> LP (158)
				> RI (109)
<i>Cluster 2 (bilateral anterior)</i>				
Left hippocampus (SUB/CA/EC)	− 22 − 14 − 24	1503	Positive (1284)	> RP (1028)
Left amygdala (LB)				= RP (392)
				> LI (838)
				= LI (728)
				> LP (1043)
				= LP (265)
				> RI (848)
				= RI (595)
Right hippocampus (CA/EC/SUB)	20 − 8 − 22	1249	Positive (1096)	> RP (1064)
Right amygdala (LB)				> LI (848)
				= LI (348)
				> LP (968)
				= LP (50)
				> RI (656)
				= RI (576)
Medial orbitofrontal cortex	4 52 − 14	445	Positive (427)	> RP (418)
				> LI (anterior 169; medial 62; posterior 36)
				> LP (anterior 148; posterior 162)
				> RI (110)
<i>Cluster 3 (left intermediate)</i>				
Left hippocampus (SUB/CA/FD)	− 22 − 24 − 16	1471	Positive (1239)	> LP (961)
Left amygdala (SF)				= LP (655)
				> Ant (1025)
				> LP (872)
				= LP (590)
				> RI (787)
				= RI (976)
Right hippocampus (SUB/CA)	22 − 22 − 16	961	Positive (858)	> RP (355)
Right amygdala (SF/LB)				= RP (491)
				> Ant (506)
				> LP (382)
				= LP (333)
				> RI (99)
				= RI (802)
Left inferior frontal, precentral gyrus	− 42 6 50	805	Negative (precentral 170)	> RP (precentral 87; IFG 36, 20)
				> Ant (500)
				> LP (precentral 66; IFG 61)

Table 1 (continued)

Cluster 1 (right posterior)	Peak voxel (X Y Z)	Size (voxels)	rsfMRI correlation	MACM contrast (voxels)	
t1.35	Supplementary motor area	−2 14 54	404	Negative (173)	= LP (145) > RI (IFG 69; precentral 24) = RI (151) > RP (61) = RP (237) > Ant (375) = LP (188) = RI (105)
t1.36	Left precuneus/retrosplenial, calcarine gyrus	−6 −56 8	280	Positive (111)	> RP (114) > Ant (184) > LP (anterior 33; posterior 25) > RI (176)
t1.37	Cluster 4 (left posterior)	−18 −32 −6	1469	Positive (1292)	> RP (812) = RP (subiculum 757; thalamus 103) > Ant (1223) > LI (915) = LI (590) > RI (subiculum 989; calcarine 30) = RI (533)
t1.38					
t1.39					
t1.40					
t1.41					
t1.42	Left calcarine gyrus				
t1.43	Right hippocampus (SUB)	20 −32 −6	544	Positive (516; 33)	= RP (483) > Ant (439)
t1.44	Right hippocampus (CA)				= Ant (265)
t1.45	Right hippocampus (FD)				> LI (222)
t1.46	Right thalamus (temporal)				= LI (333) > RI (287) = RI (267)
t1.47	SMA/MCC	2 18 40	308	Negative (22)	> Ant (261) > LI (18) = LI (188) > RI (62) = RI (69)
t1.48	Left fusiform, inferior temporal/occipital gyrus	−42 −62 −20	286	None	> RP (61) = RP (159) > Ant (218) > LI (175) > RI (124) > RP (85)
t1.49	Left inferior frontal, precentral gyrus	−42 8 30	225	Negative (187)	> Ant (216) > RI (97)
t1.50	Left calcarine, middle occipital gyrus	−8 −88 2	165	Positive (129)	> RP (100) > Ant (134) > LI (lateral 43; medial 18) > RI (69)
t1.51	Cluster 5 (right intermediate)	24 −22 −16	1403	Positive (1389)	> RP (1040) = RP (371) > Ant (957) = Ant (576) > LI (CA/subiculum 998; fusiform 119) = LI (802) > LP (1154) = LP (533)
t1.52					
t1.53					
t1.54	Left hippocampus (SUB/CA)/amygdala (LB/SF)	−22 −24 −16	1044	Positive (977)	> RP (452) = RP (559) > Ant (548) = Ant (595) > LI (16) = LI (976) > LP (330) = LP (267)
t1.55	Left precentral, middle frontal gyrus	−44 2 40	184	Negative (172)	> RP (61) > Ant (181)
t1.56	Right fusiform gyrus	44 56 −18	123	None	> RP (17) > Ant (54)
t1.57	SMA	−2 18 46	110	Negative (98)	> Ant (100) > LP (105) = LP (69) = LI (105)

680 (Supplemental Table 2; Fig. 5). In particular, the amygdala showed
681 strong rsfMRI connectivity with all subiculum subregions. In addition,
682 more anterior regions showed stronger coupling than more posterior

regions. Ventral regions of the striatum, particularly medial, were posi- 683
tively associated with anterior subiculum activity. On the other hand, 684
dorsal and middle regions of the anterior striatum were negatively 685

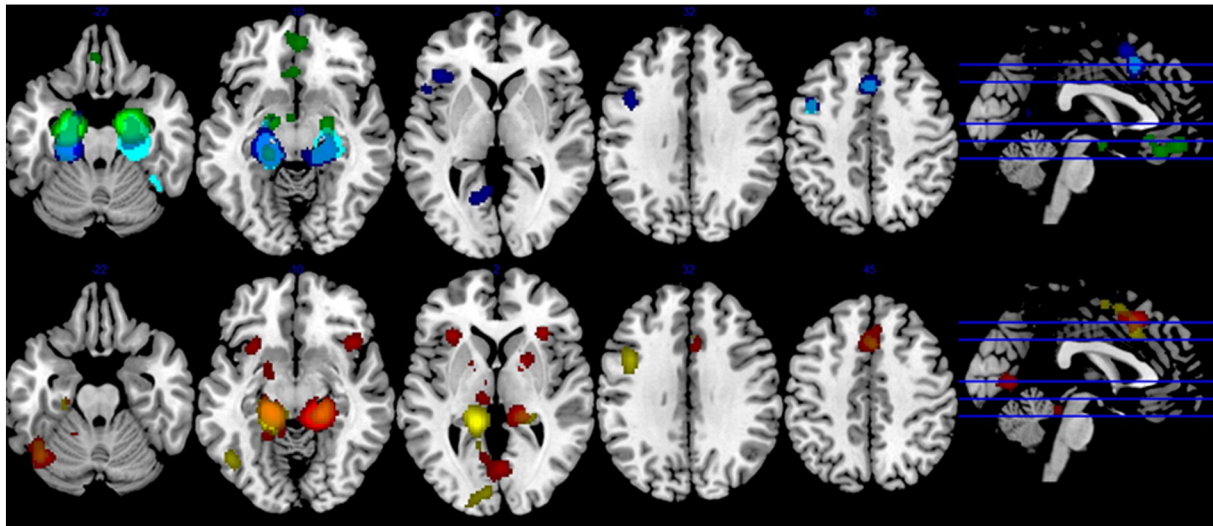


Fig. 4. Meta-analytic connectivity mapping (MACM) of each of the five subiculum subregions: top row: bilateral anterior (green); right intermediate (cyan); left intermediate (blue); bottom row: right posterior (red); left posterior (yellow). Data obtained from BrainMap database.

associated with anterior subiculum activity. In other words, activation in the anterior subiculum was associated with greater differential activation of ventral and dorsal striatum, compared to intermediate and posterior regions. Connectivity with the thalamus appeared to correspond to known anatomical connectivity, insofar as regions of the thalamus defined as connecting to the temporal lobe (on the basis of DTI connectivity (Behrens et al., 2003)) were positively associated with subiculum activity.

We were also able to investigate laterality effects in intermediate and posterior regions (Supplemental Table 2; Supplemental Fig. 5) by contrasting rsfMRI activations of the corresponding left and right subregions. In general, differential activation was observed in the ipsilateral hemisphere. However, this was sometimes seen in regions negatively correlated with the corresponding region, suggesting a reduction of anticorrelation (e.g. left dorsolateral prefrontal and inferior parietal lobule (PF/PFm): left > right intermediate). On the other hand, prominent increases were seen in the visual cortex (left > right: posterior), and ventromedial PFC and striatum (right > left: intermediate): regions, which were already positively coupled with subicular activation.

Functional characterization of subiculum subregions

Examination of the functional properties of the BrainMap database revealed that mnemonic tasks were the most reliable task to activate all subicular regions (Table 2). Among cognitive domains, explicit memory tasks activated all of the 5 subregions, and a reverse inference analysis revealed that there was a significant (above chance) probability that an explicit memory task had been administered if the subiculum was activated. Analysis of the paradigms that might be responsible revealed that cued explicit recognition paradigms, paired associates recall, episodic recall and encoding paradigms all featured larger than chance probability of activation, although not all were significant for all subregions. Reverse inference revealed that for all subregions, the presence of a subiculum activation led to a significantly increased likelihood that an encoding task had been administered. While there was little decisive evidence of mnemonic specialization within the subiculum, some variation across the region was observed. In particular, the left intermediate region generally showed the greatest likelihood of mnemonic-related activation (explicit memory and episodic recall), and was significantly more reliably associated with explicit memory than two of the four other subregions.

Activation of the subiculum was not limited to mnemonic tasks. Fear paradigms activated the anterior subiculum. There was also evidence for perceptual functions based in the subiculum: a variety of paradigms which depend on visual processing were likely to activate the region, including face monitoring and discrimination, film viewing and passive viewing. These tended to be located in anterior or intermediate regions of the subiculum compared with the posterior regions. The region, particularly the right intermediate subregion, was also engaged by the related construct of object or scene imagination.

Discussion

In the present work, we analyzed maps describing co-occurrence of significant activations across fMRI studies and used data-driven clustering to define regions with distinct patterns of co-occurring activation within the subiculum. Our K-means clustering algorithm grouped the anterior subicula from both hemispheres into one cluster. The intermediate and posterior subicula from both hemispheres were represented by distinct subregions within the left and right hemisphere, respectively. Thus, unlike the anterior region, the intermediate and posterior subiculum showed a distinct pattern of hemispheric differentiation. Altogether, we found a robust parcellation of the human subiculum consisting of five separate, functionally distinct modules, which are distributed along its antero-posterior axis. We examined two additional aspects of the subicular subregions to characterize the parcellation in greater detail. First, the functional connectivity of these five regions using resting fMRI and meta-analytic connectivity modeling (MACM) was investigated. In many cases, these patterns of connectivity or co-occurrence were compatible with anatomical relationships between the subiculum and other cortical regions described in translational studies as discussed below. Second, investigation of the functional properties of the region revealed that the subiculum was predominantly activated by mnemonic paradigms. This corroborates the established role for the region in memory, and in particular the high resolution fMRI studies that have been optimized to provide evidence of this sort (Carr et al., 2010; Suthana et al., 2011). However, there was also some evidence for a role for the region in other cognitive challenges, such as fear or perceptual paradigms. The implications of these findings for neurofunctional theories of the subiculum are likewise discussed in detail below.

The human subiculum is a relatively small structure, given the spatial resolution of fMRI, and the parcellation of the region reflected

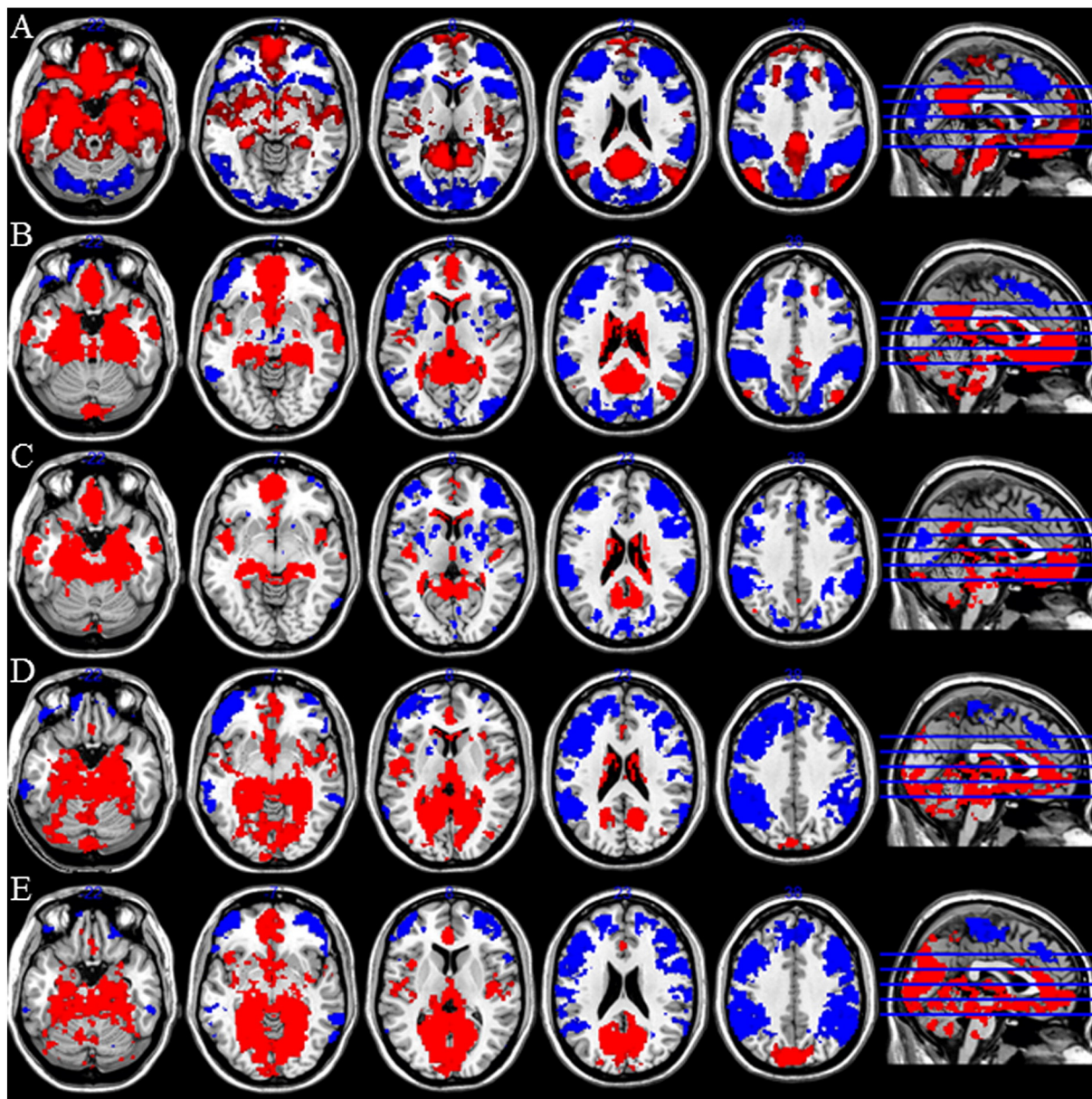


Fig. 5. Regions positively (red) and negatively (blue) connected with each subiculum subregion. Row A: anterior; row B: right intermediate; row C: left intermediate; row D: right posterior; row E: left posterior. Threshold used for display: voxelwise $p < 0.001$ uncorrected, $k = 60$. Data obtained from NKI/Rockland rsfMRI dataset.

765 information from voxels outside of the region. Nevertheless, the subre- 783
 766 gion ROIs that resulted from the clustering analysis were restricted, 784
 767 almost entirely, to the subiculum ROI defined by Amunts et al. (2005). 785
 768 Although this was not the focus of the present work, application of the 786
 769 same clustering method to the CA/DG region of the hippocampus proper 787
 770 yielded a very similar, but not identical, five cluster solution to that 788
 771 seen within the subiculum. Our interpretation of these findings is as 789
 772 follows: first, the CA/DG parcellation largely corroborates both the 790
 773 subiculum parcellation, as well as translational perspectives regarding 791
 774 long-axis specialization within the hippocampal formation (Bach et al., 792
 775 2014; Poppenk et al., 2013; Strange et al., 2014) and provide further val- 793
 776 idation of the dorso-ventral dichotomy suggested on the basis of animal 794
 777 research (Fanselow and Dong, 2010). Second, regardless of the findings, 795
 778 resolution limitations – which are particularly acute across the medial/ 796
 779 lateral dimension – would prohibit strong conclusions regarding 797
 780 separable subicular and hippocampal parcellations. Nevertheless, such 798
 781 limitations do not apply to considering hemispheric differences, nor are 799
 782 as severe across the axis of interest (anterior/posterior). We

conclude therefore that the five cluster solution may reflect a reproduc- 783
 784 ible functional motif within the hippocampal formation as a whole. Of 784
 785 course, different methodologies may reveal different patterning, as the 785
 786 degree of functional differentiation may depend on the type of physio- 786
 787 logical dimension investigated (Strange et al., 2014). As far as fMRI is 787
 788 concerned, high resolution methods are likely to be better suited to ex- 788
 789 tending our conclusion, perhaps to confirm the presence of a similar 789
 790 motif across hippocampal subregions (see also Bonnici et al., 2012). 790

Large scale brain networks: default mode and task positive networks 791

The default mode network (DMN) is a central motif of correlated, 792
 793 low frequency brain networks during rest (Raichle et al., 2001), and 793
 794 often reduces its activation during task-related, executive cognition 794
 795 (Schilbach et al., 2012). Neural activity measured with fMRI within the 795
 796 hippocampal formation is positively associated with activation of this 796
 797 network in both rodents and humans (Lu et al., 2012). Accordingly, 797
 798 we observed that resting signal fluctuations within all five subregions 798
 799

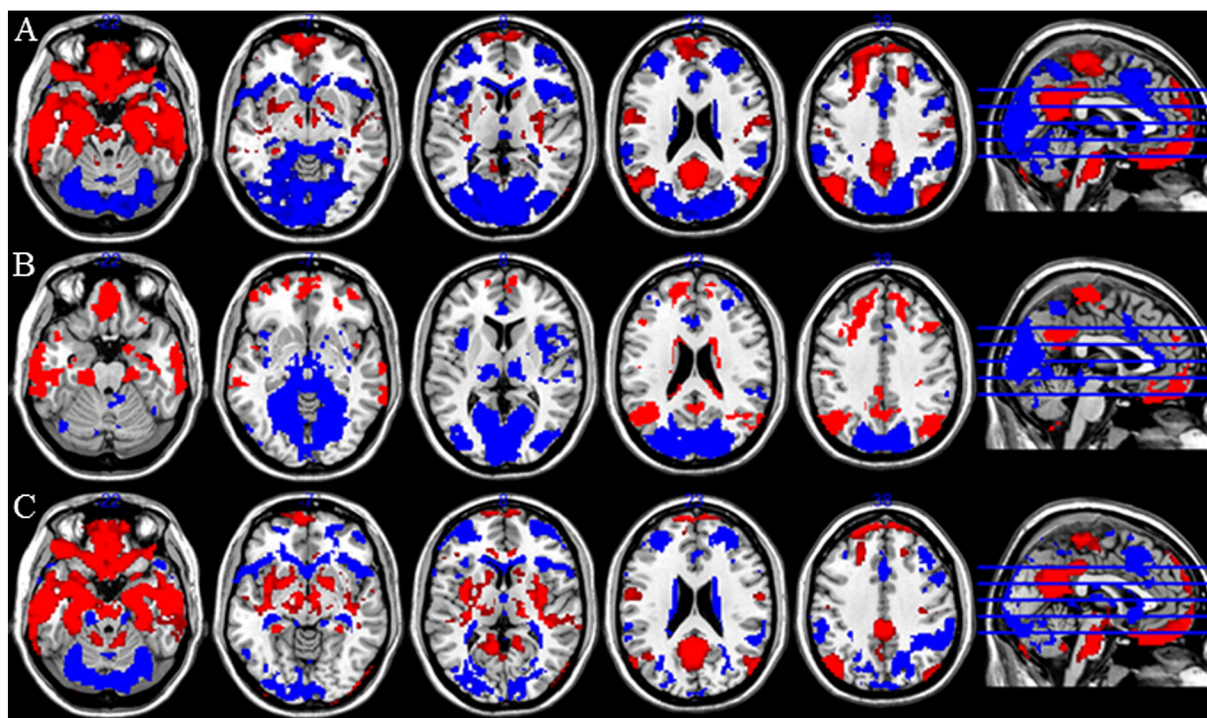


Fig. 6. Contrast between subiculum subregions. Row A: contrast of anterior and intermediate (left and right collapsed). Blue: intermediate > anterior; red: anterior > intermediate. Row B: contrast of posterior and intermediate (left and right collapsed). Blue: posterior > intermediate; red: intermediate > posterior. Row C: contrast of posterior and anterior (left and right collapsed). Blue: posterior > anterior; red: anterior > posterior. Threshold used for display: voxelwise $p < 0.001$ uncorrected, $k = 60$.

Data obtained from NKI/Rockland rsfMRI dataset.

799 of the subiculum were positively correlated with those of regions attrib- 833
 800 uted to the DMN including the rostral ACC, medial PFC (both ventral and 834
 801 dorsal), PCC and inferior parietal, and negatively correlated with those 835
 802 of ‘task positive’ regions associated with general cognitive task perfor- 836
 803 mance. Regions included in the latter category included regions associ- 837
 804 ated with executive control such as the dorsolateral PFC (Duncan and 838
 805 Owen, 2000) and intraparietal sulcus (Chamod and Petrides, 2007), 839
 806 and regions associated with sustained task performance such as the 840
 807 dorsal ACC, SMA and anterior insula (Dosenbach et al., 2006). Moreover, 841
 808 the anterior region of the subiculum was more strongly associated with 842
 809 the DMN, both in resting fMRI and MACM, while posterior and inter- 843
 810 mediate regions were comparatively more strongly associated with task 844
 811 positive regions listed above. Put another way, a more obvious anti- 845
 812 correlation between DMN and task positive networks was observed 846
 813 using more anterior rather than more posterior seeds. Given that this 847
 814 type of reciprocal relationship is arguably a characteristic of rsfMRI 848
 815 (Uddin et al., 2009), the pattern of differential connectivity in more 849
 816 anterior regions of the subiculum is therefore consistent for the most 850
 817 part with a better coupling to coherent, ongoing activation in the 851
 818 DMN. MACM provided a similar pattern of data insofar as the anterior 852
 819 subiculum was co-activated with the vmPFC, whereas intermediate 853
 820 and posterior regions were co-activated with left lateral PFC, SMA and 854
 821 anterior insula, for example. Thus, however, there was an overall bias 855
 822 toward co-occurrence of significant activations across studies with 856
 823 task positive regions, rather than a reduction of anticorrelation, as was 857
 824 seen in the rsfMRI data. It should be emphasized that the MACM analy- 858
 825 sis is not biased toward regions associated with the performance of dif- 859
 826 ficult or sustained cognition because is based on data from group 860
 827 contrast co-ordinate maps: regions associated with the DMN show 861
 828 clear ‘task’-related activation, provided the correct cognitive domain is 862
 829 examined (Schilbach et al., 2012). Rather, the evidence more clearly 863
 830 supports the notion that functional connectivity of the subiculum with 864
 831 the left lateral PFC and SMA, though not a variety of other regions (see 865
 832 Table 1), is changing substantially between task and resting states (Di

et al., 2013; Mennes et al., 2013; Messe et al., 2014). While we should 833
 acknowledge that there are potentially other interpretations of this 834
 discrepancy which do not relate directly to functional connectivity as 835
 conventionally defined (e.g. perhaps relating to task confounds), this 836
 proposed task-dependent relationship between regions is eminently 837
 testable using controlled task contexts, alternative neuroimaging meth- 838
 odologies, and statistical approaches such as dynamic causal modeling 839
 (Bernal-Casas et al., 2013) or psychophysiological interaction (Fornito 840
 et al., 2012). Indeed, we would argue that a multi-modal approach to 841
 connectivity is inevitably required to provide an adequate characteriza- 842
 tion of the functional connectivity of these regions, particularly as the 843
 MTL and PFC may communicate via distinct frequency bands (Ketz 844
 et al., 2014). 845

The posterior cingulate (PCC), which showed rsfMRI functional 846
 connectivity with all five subregions, is a key node in the default mode 847
 network, and anatomical connections between the subiculum, the PCC 848
 and nearby retrosplenial cortex (RC) are well established (Aggleton 849
 et al., 2012; Witter, 2006). It is likely that interactions between the RC 850
 and hippocampal formation play an important role in spatial memory 851
 (Albasser et al., 2007). The RC is situated slightly ventral to the posterior 852
 cingulate, and it is these connections that are likely to play a role in the 853
 substantial functional connectivity that we observed between the 854
 subiculum and specific regions within the DMN, including the inferior 855
 parietal cortex/angular gyrus and medial PFC. In the rodent, anatomical 856
 connections between the subiculum and retrosplenial cortex are 857
 relatively consistent across the entire subiculum (Aggleton et al., 858
 2012; Witter, 2006), but this contrasts with our observation that 859
 retrosplenial/subiculum functional connectivity is more robust with 860
 the anterior than posterior subiculum. One possible explanation, 861
 partially supported by the MACM findings, is that it is a consequence 862
 of stronger coupling of anterior subiculum activation with coherent 863
 DMN activity, resulting from the anterior subiculum projections to the 864
 medial prefrontal cortex (Aggleton, 2012; Witter, 2006). Thus the medi- 865
 al prefrontal cortex may mediate the statistical association between 866

Table 2

Functional properties of subiculum subregions derived from analysis of the BrainMap database. Activation given domain or paradigm reflects domains or paradigms which show above chance probability of activating the region (FDR corrected). Domain or paradigm given activation reflects reverse inference, the probability of correctly inferring a domain or paradigm from an activation (FDR corrected). Rows marked with the name of the subregion show the overall effects within the subregion, while rows marked with the regions' initials show contrasts of the regions (A = anterior; RI/LI = right/left intermediate; RP/LP = right/left posterior; region A > region B = region A shows a significantly greater likelihood of paradigm/domain-related activation than B, FDR corrected).

	Activation/domain	Domain/activation	Activation/paradigm	Paradigm/activation
t2.7				
t2.8	Anterior	Explicit memory; Fear	Explicit memory	Face monitoring/discrimination; Film viewing; Encoding
t2.9	A > RP			
t2.10	A > LI		Film viewing	
t2.11	A > LP		Face monitoring/discrimination	
t2.12	A > RI	Semantics Speech		
t2.13	Right intermediate	Explicit memory	Explicit memory	Encoding; Imagined objects; Passive viewing; Cued explicit recognition
t2.14			Cued explicit recognition; Encoding; Imagined objects/scenes; Passive viewing Imagined objects/scenes	
t2.15	RI > RP			
t2.16	RI > A	Visual perception		
t2.17	RI > LI			
t2.18	RI > LP			
t2.19	Left intermediate	Explicit memory	Explicit memory	Cued explicit recognition; Episodic recall; Encoding; Paired associates' recall;
t2.20				Cued explicit recognition; Episodic recall; Encoding; Paired associates' recall
t2.21	LI > RP	Explicit memory	Explicit memory	
t2.22	LI > A	Explicit memory	Explicit memory	Episodic recall
t2.23	LI > LP			
t2.24	LI > RI	Semantics		Episodic Recall
t2.25	Right posterior	Explicit memory	Explicit memory	Encoding; Visual distractor/attention; Go/NoGo;
t2.26	RP > A			Encoding
t2.27				
t2.28	RP > LI	Working memory		
t2.29	RP > LP			Reward task
t2.30	RP > RI	Semantics; Action execution; Speech;		Spatial location discrimination;
t2.31	Left posterior	Explicit memory	Explicit memory	Cued explicit recognition; Encoding
t2.32				Cued explicit recognition; Encoding
t2.33	LP > RP			
t2.34	LP > A	Visual perception		Visual distractor/attention
t2.35	LP > LI	Working memory; Visual perception		Film viewing
t2.36	LP > RI	Semantics		

867 activation within the anterior subiculum and the posterior cingulate
868 cortex.

869 In light of the frequent observation of activation in the subiculum
870 during memory paradigms, and the differential relationship of subicular
871 subregions with default mode and task positive networks, it is notable
872 that Fornito and colleagues (Fornito et al., 2012) demonstrated an alter-
873 ation in the inter-correlation of DMN and right lateral fronto-parietal
874 regions associated with executive cognition during a recognition mem-
875 ory paradigm. This change predicted more rapid recollection. This is
876 consistent with our findings, insofar as we observed that estimates of
877 the subiculum's functional connectivity changed dramatically from
878 task to rest conditions, such that regions of the left lateral PFC and
879 SMA were positively co-activated during task conditions but showed
880 negative coupling using rsfMRI. The Fornito et al. study implies that
881 the changes in the correlational structure of large scale networks, such
882 as the DMN, are relevant for understanding mnemonic processes (see
883 also Hermundstad et al., 2014). Moreover, the differential relationship
884 across subregions with these networks may reflect functional differ-
885 ences between the subregions. However, this will only be adequately
886 understood by examining coupling during task as well as rest conditions
887 using the same, context-dependent, within-participant estimates of
888 connectivity.

Ventral striatum and midbrain: evidence for a role in dopamine regulation 889

890 Resting fMRI revealed significant coupling between the anterior
891 subiculum subregion and ventral striatum and midbrain. Notably, how-
892 ever, anterior and posterior regions of the subiculum appeared to show
893 different patterns of connectivity with the striatum. While anterior re-
894 gions were associated with ventral regions of the striatum, this positive
895 coupling was significantly reduced in intermediate and posterior re-
896 gions. By contrast, anterior regions of the dorsal striatum were negative-
897 ly associated with the anterior subiculum, and this negative coupling
898 diminished (became less negative) with intermediate and posterior
899 seeds. Further supporting our hypotheses, midbrain activity was also
900 positively coupled with anterior subiculum. These findings are consis-
901 tent with previous investigations of interactions between hippocampus,
902 midbrain and ventral striatum identified using both resting fMRI (Kahn
903 and Shohamy, 2013) and using multimodal imaging techniques (Schott
904 et al., 2008; Stone et al., 2010). They also accord well with a role for the
905 subiculum in the regulation of dopamine neurotransmission via adjust-
906 ment of the amplitude of dopamine system responses to phasic events
907 (Lisman and Grace, 2005; Lodge and Grace, 2006).

908 Finally, we note that an association between the subiculum and ven-
909 tro-lateral striatum (putamen/pallidum) was observed in the MACM

analysis: but only for the right posterior subregion. This finding was surprising and was not consistent with evidence from rsfMRI data, in which the anterior but not posterior subiculum was connected to medial and lateral ventral striatum. It should be noted that there is evidence of a topographic projection from the subiculum to the striatum in the rodent (Groenewegen et al., 1987), where more dorsal (corresponding to posterior) subicular regions are connected to lateral striatum, and ventral (corresponding to anterior) are connected to the medial striatum. Nevertheless, it remains unclear why the co-occurrence of activations across studies in the putamen should be relatively unique to a right posterior subregion seed, and to the MACM analysis. It may be that psychological context is crucial, and thus that evidence of functional connectivity can only be found under certain task conditions. Alternatively, it may be that the BrainMap database does not provide strong representation of studies which can co-activate both the striatum and the subiculum, perhaps due to a focus in the literature of phasic reward-responses (see [Functional role of the subiculum](#) section below), although the right posterior subiculum does show a relationship with reward paradigms, albeit at an uncorrected significance level.

Connectivity with other regions: amygdala and temporal lobe

Evidence of functional connectivity between subicular subregions and amygdala was seen using both MACM and resting fMRI. We observed no evidence using MACM for a clear dissociation with regard to the amygdala, but resting fMRI revealed that anterior subiculum was more strongly connected to the amygdala than intermediate or posterior regions. These findings are consistent with anatomical evidence: connections between the subiculum and the amygdala are predominantly found within the ventral subiculum in rodents (Witter, 2006), and are bidirectional (French et al., 2003; Lipski and Grace, 2013). Important functional relationships between subiculum and ventral striatum may be controlled by amygdala (Gill and Grace, 2011, 2013).

The inter-relationship between the subiculum and the rest of the temporal lobe was not a major focus of the present study. This was due to the complex anatomical connectivity between the hippocampal formation and the temporal lobe, and the existence of differential anatomical connectivity across the proximal/distal plane of the subiculum (Aggleton, 2012). Nevertheless, our findings are compatible with previous resting fMRI studies of graded temporal lobe connectivity (Libby et al., 2012), insofar as more posterior regions of the subiculum were more strongly connected to the parahippocampal and fusiform gyri, whereas more anterior regions were more strongly connected to the perirhinal cortex and anterior temporal regions.

Thalamus

Evidence for functional connections between the subiculum and thalamus was obtained in the present work: several of the subiculum subregions were positively coupled to activity in the thalamus, although these thalamic activations were perhaps not as anterior as might be expected. Anatomical evidence strongly supports the notion that anterior regions of the thalamus should be preferentially associated with the subiculum (Aggleton et al., 1986; Saunders et al., 2005; Wright et al., 2013), connections which are thought to be crucial for memory processing (Aggleton, 2012) via interactions at theta frequency (Ketzer et al., 2014). Subicular efferents also terminate in lateral dorsal and midline thalamic nuclei, though there is relatively little input to the medial dorsal thalamus (Aggleton, 2012; Wright et al., 2013). The MACM analysis identified co-occurrence of significant activations across studies between the posterior subiculum subregions and a relatively posterior region of the thalamus. However, in general, positive subiculum/thalamus coupling in both MACM and resting fMRI corresponded to thalamic regions previously identified to be connected to the temporal lobe in a diffusion tensor imaging study (Behrens et al., 2003). Other thalamic regions showed evidence of anticorrelation with the subiculum using rsfMRI: these regions may correspond to medial dorsal regions, which

show functional and anatomical connectivity with lateral prefrontal regions subserving executive control (Alexander et al., 1986). Consequently, the anticorrelation of these thalamic regions with the subiculum may be a consequence of the anticorrelation between these lateral PFC regions and the subiculum, rather than a direct inhibitory effect exerted by the subiculum.

Prefrontal cortex and medial frontal cortex

As described previously, there was a striking difference between MACM-derived clusters using posterior and intermediate subregions of the subiculum as seeds, and the functional connectivity of these seeds measured using rsfMRI, with respect to the left lateral PFC and SMA. Importantly, functional interactions of the prefrontal cortex and hippocampal formation can be excitatory or inhibitory depending on the influence of interconnected regions such as the MD thalamus or VTA (Floresco and Grace, 2003). Thus, the different estimates of functional connectivity between subiculum and lateral PFC may be attributable to the contribution of context-dependent recruitment of other regions. By contrast, there was a more consistent positive relationship between the subiculum and vmPFC, although MACM only revealed significant co-occurrence in these regions with the anterior seed. In general, these patterns of functional connectivity reflect underlying anatomical connections. In the rodent, the ventral subiculum projects to the ventromedial prefrontal and orbitofrontal cortex (Aggleton, 2012; Witter, 2006), and homologous connections in the human may underlie the strong positive functional connectivity between the anterior subiculum and the vmPFC. Given the homology between the rodent, macaque and human DMN (Lu et al., 2012), it seems likely that similar patterns of anatomical connectivity underlie this coherent activation across species. By contrast, the dorsal subiculum of the rodent projects to the anterior cingulate cortex, although not strongly (Insausti and Munoz, 2001).

It is worth noting that co-occurrence of activations across studies between the intermediate and posterior subregions and the left lateral PFC showed some qualitative differences: the left intermediate region was characterized by relatively widespread activation that was apparent across dorsal and ventral inferior frontal gyrus, while the left posterior region showed a similar but smaller cluster, located centrally within the same region of dorsolateral PFC. By contrast, the right posterior subregion had no co-occurrence across studies in the left PFC, and the right intermediate subregion only a discrete locus in a dorsal region, within the premotor cortex. These findings are intriguing as a similar region of left lateral PFC is reliably associated with the emotional modulation of explicit memory encoding (Murty et al., 2010), and supports the existence of a functional pathway between the left lateral PFC and subiculum. Indeed, the left intermediate subregion showed both the largest co-occurrence across studies in left lateral PFC, as well as the most reliable association with explicit memory using BrainMap.

Hemispheric lateralization of intermediate and posterior regions

Our findings, both the parcellation and the connectivity analyses, provide clear support for evidence of a hemispheric differentiation of function in the MTL (e.g. Kelley et al., 1998; Kennepohl et al., 2007; Suthana et al., 2011). However, the fact that hemispheric differences are only seen in the posterior and intermediate regions would not necessarily have been a strong prediction. This observation may relate to the general interpretation of anterior/posterior differences in the subiculum: that more posterior regions are better connected to lateral prefrontal regions that would also be expected to show hemispheric differences (e.g. Habib et al., 2003).

To follow up the result of the parcellation, we performed contrasts of the rsfMRI data between the left and right subregions of the intermediate and posterior subiculum. Although, often more positive ipsilateral coupling was observed, as might be expected, there were some intriguing differences which suggest differential hemispheric coupling with

1036 large scale brain networks, including structures such as the ventro-
 1037 medial PFC (intermediate right > left), left dorsolateral PFC and in-
 1038 ferior parietal lobule (PF) (intermediate left > right) or visual cortex
 1039 (posterior left > right). Indeed, Andrews-Hanna and colleagues
 1040 (Andrews-Hanna et al., 2010a, 2010b) have emphasized interactions
 1041 between the MTL and the DMN in the kinds of ongoing, unconstrained
 1042 cognitions – particularly mental time travel – that would occur during
 1043 rsfMRI acquisition. It may be that the right subiculum, particularly the
 1044 intermediate region which showed stronger functional connectivity
 1045 with the vmPFC, is more readily integrated into this spontaneous,
 1046 unconstrained cognition network than subregions on the left. This pro-
 1047 posal could potentially be tested (Andrews-Hanna et al., 2010a). In this
 1048 light, it is notable that the right intermediate subregion was also found
 1049 to be most consistently related to imagination of objects or scenes, a
 1050 finding with potential relevance for understanding the content of cogni-
 1051 tion during the resting state.

1052 *Functional role of the subiculum*

1053 Analysis of the functional role of the subregions largely supported
 1054 the view that the MTL is engaged by memory paradigms (Henson,
 1055 2005). Although there was some support for a role for the region in
 1056 other domains of cognition (e.g. face perception, imagination, film view-
 1057 ing), many of these may rely on or engage similar processes as those on
 1058 which episodic memory depends: for example, the ability to construct
 1059 scenes internally or other visual imagery (Hassabis and Maguire,
 1060 2007). Indeed, the observation that aspects of visual cognition may de-
 1061 pend on the subiculum is relevant to a debate regarding the relative im-
 1062 portance of the hippocampal formation's role in mnemonic and visual
 1063 processing (Buckley, 2005). Pertinent to this debate, constructs relating
 1064 to visual processing tended to be most dependent on anterior and inter-
 1065 mediate regions rather than posterior regions. Notably these regions are
 1066 connected with the perirhinal region (Aggleton, 2012; Libby et al.,
 1067 2012), and evidence for the perirhinal cortex in perceptual processes
 1068 is gradually emerging (e.g. Barense et al., 2012).

1069 In general however, in contrast to our functional connectivity analy-
 1070 ses, the functional decoding analysis yielded relatively little strong
 1071 support for the notion that there may be functional differences across
 1072 the anterior/posterior extent of the subiculum. However, it is neverthe-
 1073 less worth noting that fear paradigms were likely to activate the anteri-
 1074 or subiculum, consistent for a role for the subregion in emotional or
 1075 stress-related behavior (Herman and Mueller, 2006; Lowry, 2002;
 1076 Valenti et al., 2011), and also with the strong anatomical connectivity
 1077 with the amygdala (French et al., 2003). Indeed, the dual activation of
 1078 the anterior subiculum by episodic memory paradigms and emotional
 1079 stimuli is consistent with the view that it may play a role in determining
 1080 an emotional or motivational context for behavior (Grace, 2010), and
 1081 accords with theoretical perspectives regarding emotion as a mnemonic
 1082 contextual signal (e.g. Bower, 1981).

1083 Although the Brain Map database is comprehensive and as unbiased
 1084 a resource as may be expected, there may be areas in which publication
 1085 biases are manifest (e.g. task confounds correlated with a particular
 1086 paradigm class c.f. Poppenk et al., 2013). These may also be particularly
 1087 relevant for paradigms, such as stress, in which a rather complex inter-
 1088 action of elements of experimental design may be necessary. In addi-
 1089 tion, the involvement of the subiculum in reward and motivated
 1090 behavior, which is established in rodent studies (Sesack and Grace,
 1091 2010), was not strongly confirmed in the functional characterization
 1092 analysis (with a possible exception of the right posterior subregion at
 1093 an uncorrected threshold). A possible cause may relate to a focus of
 1094 reward-related fMRI studies on phasic reward responses that engage
 1095 the ventral striatum, whereas the subiculum may provide a greater con-
 1096 tribution to tonic, context-related motivational signals (Grace, 2012;
 1097 Lisman and Grace, 2005). There was also no clear evidence for function-
 1098 al differences between hemispheres, as has been suggested for the
 1099 hippocampus (e.g. Kelley et al., 1998; Kennepohl et al., 2007; but see

Henson, 2005), for example, in terms of encoding and retrieval as has
 been specifically suggested for the subiculum (Carr et al., 2010;
 Suthana et al., 2011). Nevertheless, the left intermediate region showed
 particularly reliable memory related activation, which may reflect an
 underlying specialization for the region. It is likely that the taxonomy
 employed by the BrainMap database may not be of a sufficient resolu-
 tion to clarify more fully the functional role of subicular subregions, as
 potentially relevant differences such as the content of memory
 encoding (Kennepohl et al., 2007) or attentional influences (Carr et al.,
 2013) are not coded.

Summary

An overriding theme of the present work is that the information
 about the subiculum's anatomical and functional connectivity derived
 predominantly from research with experimental animals is, in many
 ways, comparable to that obtained using functional neuroimaging
 methods (Strange et al., 2014). Our findings point support organization-
 al framework for the human hippocampus – that of an anterior–
 posterior differentiation of function, which may guide further transla-
 tional research. This organization reveals different relationships across
 the structure with regions subserving executive and sustained cogni-
 tion, and the default mode networks, with posterior and intermediate
 regions being more strongly related to the former regions, and the an-
 terior region to the DMN. Posterior and intermediate regions were distin-
 guished from each other by differential connectivity with the left lateral
 PFC, and discrete loci within occipital and temporal regions. The right
 posterior subregion was related to putamen activation and also showed
 an (uncorrected) relationship with reward paradigms. Our findings
 provided strong support for a role for the subiculum in memory para-
 digms, and some evidence for a contribution in perceptual and emo-
 tional processes, although we found little consistent evidence for a
 neurofunctional dissociations of this region using the BrainMap taxon-
 omies. The five cluster model may be useful as a means of clarifying
 distinct pathological pathways underlying disease states, which we an-
 ticipate will be an area of future interest due to the role of the region in
 the contextual control of behavior and the endocrine response to stress.

Funding

This study was supported by the National Institute of Mental Health
 (NIMH) grant R01 MH076971 (to M.L.P.)

Conflicts of interest

None of the authors declare any financial or other conflicts of inter-
 est that might have biased the work.

Appendix A. Supplementary data

Supplementary data to this article can be found online at <http://dx.doi.org/10.1016/j.neuroimage.2015.02.069>.

References

- Aggleton, J.P., 2012. Multiple anatomical systems embedded within the primate medial temporal lobe: implications for hippocampal function. *Neurosci. Biobehav. Rev.* 36, 1579–1596.
- Aggleton, J.P., Desimone, R., Mishkin, M., 1986. The origin, course, and termination of the hippocampothalamic projections in the macaque. *J. Comp. Neurol.* 243, 409–421.
- Aggleton, J.P., Wright, N.F., Vann, S.D., Saunders, R.C., 2012. Medial temporal lobe projections to the retrosplenial cortex of the macaque monkey. *Hippocampus* 22, 1883–1900.
- Albasser, M.M., Poirier, G.L., Warburton, E.C., Aggleton, J.P., 2007. Hippocampal lesions halve immediate-early gene protein counts in retrosplenial cortex: distal dysfunctions in a spatial memory system. *Eur. J. Neurosci.* 26, 1254–1266.
- Alexander, G.E., DeLong, M.R., Strick, P.L., 1986. Parallel organization of functionally segregated circuits linking basal ganglia and cortex. *Annu. Rev. Neurosci.* 9, 357–381.
- Amunts, K., Kedo, O., Kindler, M., Pieperhoff, P., Mohlberg, H., Shah, N.J., Habel, U., Schneider, F., Zilles, K., 2005. Cytoarchitectonic mapping of the human amygdala,

- hippocampal region and entorhinal cortex: intersubject variability and probability maps. *Anat. Embryol. (Berl.)* 210, 343–352.
- Andrews-Hanna, J.R., Reidler, J.S., Huang, C., Buckner, R.L., 2010a. Evidence for the default network's role in spontaneous cognition. *J. Neurophysiol.* 104, 322–335.
- Andrews-Hanna, J.R., Reidler, J.S., Sepulcre, J., Poulin, R., Buckner, R.L., 2010b. Functional-anatomic fractionation of the brain's default network. *Neuron* 65, 550–562.
- Andrzejewski, M.E., Spencer, R.C., Kelley, A.E., 2006. Dissociating ventral and dorsal subicular dopamine D1 receptor involvement in instrumental learning, spontaneous motor behavior, and motivation. *Behav. Neurosci.* 120, 542–553.
- Ashburner, J., Friston, K.J., 2005. Unified segmentation. *Neuroimage* 26, 839–851.
- Bach, D.R., Guitart-Masip, M., Packard, P.A., Miro, J., Falip, M., Fuentemilla, L., Dolan, R.J., 2014. Human hippocampus arbitrates approach-avoidance conflict. *Curr. Biol.* 24, 541–547.
- Bannerman, D.M., Sprengel, R., Sanderson, D.J., McHugh, S.B., Rawlins, J.N., Monyer, H., Seeburg, P.H., 2014. Hippocampal synaptic plasticity, spatial memory and anxiety. *Nat. Rev. Neurosci.* 15, 181–192.
- Barense, M.D., Groen, I.I., Lee, A.C., Yeung, L.K., Brady, S.M., Gregori, M., Kapur, N., Bussey, T.J., Saksida, L.M., Henson, R.N., 2012. Intact memory for irrelevant information impairs perception in amnesia. *Neuron* 75, 157–167.
- Baria, A.T., Mansour, A., Huang, L., Baiiki, M.N., Cecchi, G.A., Mesulam, M.M., Apkarian, A.V., 2013. Linking human brain local activity fluctuations to structural and functional network architectures. *Neuroimage* 73, 144–155.
- Bartels, A., Logothetis, N.K., Moutoussis, K., 2008. fMRI and its interpretations: an illustration on directional selectivity in area V5/MT. *Trends Neurosci.* 31, 444–453.
- Baumann, O., Mattingley, J.B., 2013. Dissociable representations of environmental size and complexity in the human hippocampus. *J. Neurosci.* 33, 10526–10533.
- Behrens, T.E., Johansen-Berg, H., Woolrich, M.W., Smith, S.M., Wheeler-Kingshott, C.A., Boulby, P.A., Barker, G.J., Sillery, E.L., Sheehan, K., Ciccarelli, O., Thompson, A.J., Brady, J.M., Matthews, P.M., 2003. Non-invasive mapping of connections between human thalamus and cortex using diffusion imaging. *Nat. Neurosci.* 6, 750–757.
- Belujon, P., Grace, A.A., 2008. Critical role of the prefrontal cortex in the regulation of hippocampus-accumbens information flow. *J. Neurosci.* 28, 9797–9805.
- Belujon, P., Grace, A.A., 2014. Restoring mood balance in depression: ketamine reverses deficit in dopamine-dependent synaptic plasticity. *Biol. Psychiatry*.
- Bernal-Casas, D., Balaguer-Ballester, E., Gerchen, M.F., Iglesias, S., Walter, H., Heinz, A., Meyer-Lindenberg, A., Stephan, K.E., Kirsch, P., 2013. Multi-site reproducibility of prefrontal-hippocampal connectivity estimates by stochastic DCM. *Neuroimage* 82, 555–563.
- Bonnici, H.M., Chadwick, M.J., Kumaran, D., Hassabis, D., Weiskopf, N., Maguire, E.A., 2012. Multi-voxel pattern analysis in human hippocampal subfields. *Front. Hum. Neurosci.* 6, 290.
- Bower, G.H., 1981. Mood and memory. *Am. Psychol.* 36, 129–148.
- Buckley, M.J., 2005. The role of the perirhinal cortex and hippocampus in learning, memory, and perception. *Q. J. Exp. Psychol. B* 58, 246–268.
- Bzdok, D., Laird, A.R., Zilles, K., Fox, P.T., Eickhoff, S.B., 2012. An investigation of the structural, connective, and functional subspecialization in the human amygdala. *Hum. Brain Mapp.*
- Bzdok, D., Langner, R., Schilbach, L., Jakobs, O., Roski, C., Caspers, S., Laird, A.R., Fox, P.T., Zilles, K., Eickhoff, S.B., 2013. Characterization of the temporo-parietal junction by combining data-driven parcellation, complementary connectivity analyses, and functional decoding. *Neuroimage* 81, 381–392.
- Caine, S.B., Humby, T., Robbins, T.W., Everitt, B.J., 2001. Behavioral effects of psychomotor stimulants in rats with dorsal and ventral subiculum lesions: locomotion, cocaine self-administration, and prepulse inhibition of startle. *Behav. Neurosci.* 115, 880–894.
- Carr, V.A., Rissman, J., Wagner, A.D., 2010. Imaging the human medial temporal lobe with high-resolution fMRI. *Neuron* 65, 298–308.
- Carr, V.A., Engel, S.A., Knowlton, B.J., 2013. Top-down modulation of hippocampal encoding activity as measured by high-resolution MRI. *Neuropsychologia* 51, 1829–1837.
- Caspers, S., Zilles, K., Laird, A.R., Eickhoff, S.B., 2010. ALE meta-analysis of action observation and imitation in the human brain. *Neuroimage* 50, 1148–1167.
- Chamod, A.S., Petrides, M., 2007. Dissociable roles of the posterior parietal and the prefrontal cortex in manipulation and monitoring processes. *Proc. Natl. Acad. Sci. U. S. A.* 104, 14837–14842.
- Cieslik, E.C., Zilles, K., Caspers, S., Roski, C., Kellermann, T.S., Jakobs, O., Langner, R., Laird, A.R., Fox, P.T., Eickhoff, S.B., 2013. Is there “One” DLPFC in cognitive action control? Evidence for heterogeneity from co-activation-based parcellation. *Cereb. Cortex* 23, 2677–2689.
- Clos, M., Amunts, K., Laird, A.R., Fox, P.T., Eickhoff, S.B., 2013. Tackling the multifunctional nature of Broca's region meta-analytically: co-activation-based parcellation of area 44. *Neuroimage* 83C, 174–188.
- Clos, M., Rottschy, C., Laird, A.R., Fox, P.T., Eickhoff, S.B., 2014. Comparison of structural covariance with functional connectivity approaches exemplified by an investigation of the left anterior insula. *Neuroimage* 99, 269–280.
- Crossley, N.A., Mechelli, A., Vertes, P.E., Winton-Brown, T.T., Patel, A.X., Ginestet, C.E., McGuire, P., Bullmore, E.T., 2013. Cognitive relevance of the community structure of the human brain functional coactivation network. *Proc. Natl. Acad. Sci. U. S. A.* 110, 11583–11588.
- Damoiseaux, J.S., Greicius, M.D., 2009. Greater than the sum of its parts: a review of studies combining structural connectivity and resting-state functional connectivity. *Brain Struct. Funct.* 213, 525–533.
- Di, X., Gohel, S., Kim, E.H., Biswal, B.B., 2013. Task vs. rest-different network configurations between the coactivation and the resting-state brain networks. *Front. Hum. Neurosci.* 7, 493.
- Dosenbach, N.U., Visscher, K.M., Palmer, E.D., Miezin, F.M., Wenger, K.K., Kang, H.C., Burgund, E.D., Grimes, A.L., Schlaggar, B.L., Petersen, S.E., 2006. A core system for the implementation of task sets. *Neuron* 50, 799–812.
- Duncan, J., Owen, A.M., 2000. Common regions of the human frontal lobe recruited by diverse cognitive demands. *Trends Neurosci.* 23, 475–483.
- Duvernoy, H.M., 2005. The Human Hippocampus: Functional Anatomy, Vascularization, and Serial Sections with MRI. Third ed. Springer, Berlin; New York.
- Eickhoff, S.B., Stephan, K.E., Mohlberg, H., Grefkes, C., Fink, G.R., Amunts, K., Zilles, K., 2005. A new SPM toolbox for combining probabilistic cytoarchitectonic maps and functional imaging data. *Neuroimage* 25, 1325–1335.
- Eickhoff, S.B., Laird, A.R., Grefkes, C., Wang, L.E., Zilles, K., Fox, P.T., 2009. Coordinate-based activation likelihood estimation meta-analysis of neuroimaging data: a random-effects approach based on empirical estimates of spatial uncertainty. *Hum. Brain Mapp.* 30, 2907–2926.
- Eickhoff, S.B., Bzdok, D., Laird, A.R., Roski, C., Caspers, S., Zilles, K., Fox, P.T., 2011. Co-activation patterns distinguish cortical modules, their connectivity and functional differentiation. *Neuroimage* 57, 938–949.
- Eickhoff, S.B., Bzdok, D., Laird, A.R., Kurth, F., Fox, P.T., 2012. Activation likelihood estimation meta-analysis revisited. *Neuroimage* 59, 2349–2361.
- Eickhoff, S.B., Laird, A.R., Fox, P.T., Bzdok, D., Hensel, L., 2014. Functional segregation of the human dorsomedial prefrontal cortex. *Cereb. Cortex*.
- Fanselow, M.S., Dong, H.W., 2010. Are the dorsal and ventral hippocampus functionally distinct structures? *Neuron* 65, 7–19.
- Floresco, S.B., Grace, A.A., 2003. Gating of hippocampal-evoked activity in prefrontal cortical neurons by inputs from the mediadorsal thalamus and ventral tegmental area. *J. Neurosci.* 23, 3930–3943.
- Fornito, A., Harrison, B.J., Zalesky, A., Simons, J.S., 2012. Competitive and cooperative dynamics of large-scale brain functional networks supporting recollection. *Proc. Natl. Acad. Sci. U. S. A.* 109, 12788–12793.
- Fox, P.T., Lancaster, J.L., 2002. Opinion: mapping context and content: the BrainMap model. *Nat. Rev. Neurosci.* 3, 319–321.
- French, S.J., Hailstone, J.C., Totterdell, S., 2003. Basolateral amygdala efferents to the ventral subiculum preferentially innervate pyramidal cell dendritic spines. *Brain Res.* 981, 160–167.
- Gill, K.M., Grace, A.A., 2011. Heterogeneous processing of amygdala and hippocampal inputs in the rostral and caudal subregions of the nucleus accumbens. *Int. J. Neuropsychopharmacol.* 14, 1301–1314.
- Gill, K.M., Grace, A.A., 2013. Differential effects of acute and repeated stress on hippocampus and amygdala inputs to the nucleus accumbens shell. *Int. J. Neuropsychopharmacol.* 16, 2013–2025.
- Grace, A.A., 2010. Dopamine system dysregulation by the ventral subiculum as the common pathophysiological basis for schizophrenia psychosis, psychostimulant abuse, and stress. *Neurotox. Res.* 18, 367–376.
- Grace, A.A., 2012. Dopamine system dysregulation by the hippocampus: implications for the pathophysiology and treatment of schizophrenia. *Neuropharmacology* 62, 1342–1348.
- Groenewegen, H.J., Vermeulen-Van der Zee, E., te Kortschot, A., Witter, M.P., 1987. Organization of the projections from the subiculum to the ventral striatum in the rat. A study using anterograde transport of *Phaseolus vulgaris* leucoagglutinin. *Neuroscience* 23, 103–120.
- Habib, R., Nyberg, L., Tulving, E., 2003. Hemispheric asymmetries of memory: the HERA model revisited. *Trends Cogn. Sci.* 7, 241–245.
- Hartigan, J.A., Wong, M.A., 1979. A k-means clustering algorithm. *Appl. Stat.* 28, 100–108.
- Hassabis, D., Maguire, E.A., 2007. Deconstructing episodic memory with construction. *Trends Cogn. Sci.* 11, 299–306.
- Henson, R., 2005. A mini-review of fMRI studies of human medial temporal lobe activity associated with recognition memory. *Q. J. Exp. Psychol. B* 58, 340–360.
- Herman, J.P., Mueller, N.K., 2006. Role of the ventral subiculum in stress integration. *Behav. Brain Res.* 174, 215–224.
- Hermundstad, A.M., Brown, K.S., Bassett, D.S., Aminoff, E.M., Frithsen, A., Johnson, A., Tipper, C.M., Miller, M.B., Grafton, S.T., Carlson, J.M., 2014. Structurally-constrained relationships between cognitive states in the human brain. *PLoS Comput. Biol.* 10, e1003591.
- Hirshhorn, M., Grady, C., Rosenbaum, R.S., Winocur, G., Moscovitch, M., 2012. Brain regions involved in the retrieval of spatial and episodic details associated with a familiar environment: an fMRI study. *Neuropsychologia* 50, 3094–3106.
- Insausti, R., Munoz, M., 2001. Cortical projections of the non-entorhinal hippocampal formation in the cynomolgus monkey (*Macaca fascicularis*). *Eur. J. Neurosci.* 14, 435–451.
- Jakobs, O., Langner, R., Caspers, S., Roski, C., Cieslik, E.C., Zilles, K., Laird, A.R., Fox, P.T., Eickhoff, S.B., 2012. Across-study and within-subject functional connectivity of a right temporo-parietal junction subregion involved in stimulus-context integration. *Neuroimage* 60, 2389–2398.
- Kahn, I., Shohamy, D., 2013. Intrinsic connectivity between the hippocampus, nucleus accumbens, and ventral tegmental area in humans. *Hippocampus* 23, 187–192.
- Kahnt, T., Chang, L.J., Park, S.Q., Heinzle, J., Haynes, J.D., 2012. Connectivity-based parcellation of the human orbitofrontal cortex. *J. Neurosci.* 32, 6240–6250.
- Kelley, W.M., Miezin, F.M., McDermott, K.B., Buckner, R.L., Raichle, M.E., Cohen, N.J., Ollinger, J.M., Akbudak, E., Conturo, T.E., Snyder, A.Z., Petersen, S.E., 1998. Hemispheric specialization in human dorsal frontal cortex and medial temporal lobe for verbal and nonverbal memory encoding. *Neuron* 20, 927–936.
- Kennepohl, S., Sziklas, V., Garver, K.E., Wagner, D.D., Jones-Gotman, M., 2007. Memory and the medial temporal lobe: hemispheric specialization reconsidered. *Neuroimage* 36, 969–978.
- Ketz, N.A., Jensen, O., O'Reilly, R.C., 2014. Thalamic pathways underlying prefrontal cortex-medial temporal lobe oscillatory interactions. *Trends Neurosci.*
- Kuhn, S., Gallinat, J., 2014. Segregating cognitive functions within hippocampal formation: a quantitative meta-analysis on spatial navigation and episodic memory. *Hum. Brain Mapp.* 35, 1129–1142.

- 1331 Laird, A.R., Eickhoff, S.B., Fox, P.M., Uecker, A.M., Ray, K.L., Saenz Jr., J.J., McKay, D.R., Bzdok,
1332 D., Laird, R.W., Robinson, J.L., Turner, J.A., Turkeltaub, P.E., Lancaster, J.L., Fox, P.T.,
1333 2011. The BrainMap strategy for standardization, sharing, and meta-analysis of neuro-
1334 imaging data. *BMC Res Notes* 4, 349.
- 1335 Libby, L.A., Ekstrom, A.D., Ragland, J.D., Ranganath, C., 2012. Differential connectivity of
1336 perirhinal and parahippocampal cortices within human hippocampal subregions re-
1337 vealed by high-resolution functional imaging. *J. Neurosci.* 32, 6550–6560.
- 1338 Lipski, W.J., Grace, A.A., 2013. Footshock-induced responses in ventral subiculum neurons
1339 are mediated by locus coeruleus noradrenergic afferents. *Eur. Neuropsychopharmacol.*
1340 23, 1320–1328.
- 1341 Lisman, J.E., Grace, A.A., 2005. The hippocampal–VTA loop: controlling the entry of infor-
1342 mation into long-term memory. *Neuron* 46, 703–713.
- 1343 Lodge, D.J., Grace, A.A., 2006. The hippocampus modulates dopamine neuron responsivity
1344 by regulating the intensity of phasic neuron activation. *Neuropsychopharmacology*
1345 31, 1356–1361.
- 1346 Lodge, D.J., Grace, A.A., 2008. Amphetamine activation of hippocampal drive of mesolimbic
1347 dopamine neurons: a mechanism of behavioral sensitization. *J. Neurosci.* 28, 7876–7882.
- 1348 Lodge, D.J., Grace, A.A., 2011. Hippocampal dysregulation of dopamine system function
1349 and the pathophysiology of schizophrenia. *Trends Pharmacol. Sci.* 32, 507–513.
- 1350 Lowry, C.A., 2002. Functional subsets of serotonergic neurones: implications for control of
1351 the hypothalamic–pituitary–adrenal axis. *J. Neuroendocrinol.* 14, 911–923.
- 1352 Lu, H., Zou, Q., Gu, H., Raichle, M.E., Stein, E.A., Yang, Y., 2012. Rat brains also have a default
1353 mode network. *Proc. Natl. Acad. Sci. U. S. A.* 109, 3979–3984.
- 1354 Meila, M., 2007. Comparing clusterings – an information based distance. *J. Multivar. Anal.*
1355 98, 873–895.
- 1356 Mennes, M., Kelly, C., Colcombe, S., Castellanos, F.X., Milham, M.P., 2013. The extrinsic and
1357 intrinsic functional architectures of the human brain are not equivalent. *Cereb. Cortex*
1358 23, 223–229.
- 1359 Messe, A., Rudrauf, D., Benali, H., Marrelec, G., 2014. Relating structure and function in the
1360 human brain: relative contributions of anatomy, stationary dynamics, and non-
1361 stationarities. *PLoS Comput. Biol.* 10, e1003530.
- 1362 Murty, V.P., Ritchey, M., Adcock, R.A., LaBar, K.S., 2010. fMRI studies of successful emotion-
1363 al memory encoding: a quantitative meta-analysis. *Neuropsychologia* 48, 3459–3469.
- 1364 Naber, P.A., Witter, M.P., Lopes Silva, F.H., 2000. Networks of the hippocampal memory
1365 system of the rat. The pivotal role of the subiculum. *Ann. N. Y. Acad. Sci.* 911,
1366 392–403.
- 1367 Nadel, L., Hoescheidt, S., Ryan, L.R., 2013. Spatial cognition and the hippocampus: the anter-
1368 ior–posterior axis. *J. Cogn. Neurosci.* 25, 22–28.
- 1369 O'Mara, S., 2006. Controlling hippocampal output: the central role of subiculum in hippo-
1370 campal information processing. *Behav. Brain Res.* 174, 304–312.
- 1371 Poppenk, J., Evensmoen, H.R., Moscovitch, M., Nadel, L., 2013. Long-axis specialization of
1372 the human hippocampus. *Trends Cogn. Sci.* 17, 230–240.
- 1373 Raichle, M.E., MacLeod, A.M., Snyder, A.Z., Powers, W.J., Gusnard, D.A., Shulman, G.L.,
1374 2001. A default mode of brain function. *Proc. Natl. Acad. Sci. U. S. A.* 98, 676–682.
- 1375 Rottschy, C., Caspers, S., Roski, C., Retz, K., Dogan, I., Schulz, J.B., Zilles, K., Laird, A.R., Fox,
1376 P.T., Eickhoff, S.B., 2013. Differentiated parietal connectivity of frontal regions for
1377 “what” and “where” memory. *Brain Struct. Funct.* 218, 1551–1567.
- 1378 Satterthwaite, T.D., Wolf, D.H., Loughhead, J., Ruparel, K., Elliott, M.A., Hakonarson, H., Gur,
1379 R.C., Gur, R.E., 2012. Impact of in-scanner head motion on multiple measures of func-
1380 tional connectivity: relevance for studies of neurodevelopment in youth. *Neuroimage*
1381 60, 623–632.
- Saunders, R.C., Mishkin, M., Aggleton, J.P., 2005. Projections from the entorhinal cortex, 1382
perirhinal cortex, presubiculum, and parasubiculum to the medial thalamus in ma- 1383
caque monkeys: identifying different pathways using disconnection techniques. 1384
Exp. Brain Res. 167, 1–16. 1385
- Schilbach, L., Bzdok, D., Timmermans, B., Fox, P.T., Laird, A.R., Vogeley, K., Eickhoff, S.B., 1386
2012. Introspective minds: using ALE meta-analyses to study commonalities in the 1387
neural correlates of emotional processing, social & unconstrained cognition. *PLoS* 1388
ONE 7, e30920. 1389
- Schott, B.H., Minuzzi, L., Krebs, R.M., Elmenhorst, D., Lang, M., Winz, O.H., Seidenbecher, 1390
C.I., Coenen, H.H., Heinze, H.J., Zilles, K., Duzel, E., Bauer, A., 2008. Mesolimbic func- 1391
tional magnetic resonance imaging activations during reward anticipation correlate 1392
with reward-related ventral striatal dopamine release. *J. Neurosci.* 28, 14311–14319. 1393
- Sesack, S.R., Grace, A.A., 2010. Cortico-basal ganglia reward network: microcircuitry. 1394
Neuropsychopharmacology 35, 27–47. 1395
- Stone, J.M., Howes, O.D., Egerton, A., Kambeitz, J., Allen, P., Lythgoe, D.J., O'Gorman, R.L., 1396
McLean, M.A., Barker, G.J., McGuire, P., 2010. Altered relationship between hippocam- 1397
pal glutamate levels and striatal dopamine function in subjects at ultra high risk of 1398
psychosis. *Biol. Psychiatry* 68, 599–602. 1399
- Strange, B.A., Fletcher, P.C., Henson, R.N., Friston, K.J., Dolan, R.J., 1999. Segregating the 1400
functions of human hippocampus. *Proc. Natl. Acad. Sci. U. S. A.* 96, 4034–4039. 1401
- Strange, B.A., Witter, M.P., Lein, E.S., Moser, E.I., 2014. Functional organization of the hip- 1402
pocampal longitudinal axis. *Nat. Rev. Neurosci.* 15, 655–669. 1403
- Suthana, N., Ekstrom, A., Moshirvaziri, S., Knowlton, B., Bookheimer, S., 2011. Dissocia- 1404
tions within human hippocampal subregions during encoding and retrieval of spatial 1405
information. *Hippocampus* 21, 694–701. 1406
- Turkeltaub, P.E., Eden, G.F., Jones, K.M., Zeffiro, T.A., 2002. Meta-analysis of the functional 1407
neuroanatomy of single-word reading: method and validation. *Neuroimage* 16, 1408
765–780. 1409
- Turkeltaub, P.E., Eickhoff, S.B., Laird, A.R., Fox, M., Wiener, M., Fox, P., 2012. Minimizing 1410
within-experiment and within-group effects in Activation Likelihood Estimation 1411
meta-analyses. *Hum. Brain Mapp.* 33, 1–13. 1412
- Uddin, L.Q., Kelly, A.M., Biswal, B.B., Castellanos, F.X., Milham, M.P., 2009. Functional con- 1413
nectivity of default mode network components: correlation, anticorrelation, and cau- 1414
sality. *Hum. Brain Mapp.* 30, 625–637. 1415
- Valenti, O., Lodge, D.J., Grace, A.A., 2011. Aversive stimuli alter ventral tegmental area do- 1416
pamine neuron activity via a common action in the ventral hippocampus. *J. Neurosci.* 1417
31, 4280–4289. 1418
- Van Dijk, K.R., Hedden, T., Venkataraman, A., Evans, K.C., Lazar, S.W., Buckner, R.L., 2010. 1419
Intrinsic functional connectivity as a tool for human connectomics: theory, proper- 1420
ties, and optimization. *J. Neurophysiol.* 103, 297–321. 1421
- Voets, N.L., Zamboni, G., Stokes, M.G., Carpenter, K., Stacey, R., Adcock, J.E., 2014. Aberrant 1422
functional connectivity in dissociable hippocampal networks is associated with defi- 1423
cits in memory. *J. Neurosci.* 34, 4920–4928. 1424
- Voorn, P., Vanderschuren, L.J., Groenewegen, H.J., Robbins, T.W., Pennartz, C.M., 2004. Put- 1425
ting a spin on the dorsal–ventral divide of the striatum. *Trends Neurosci.* 27, 1426
468–474. 1427
- Witter, M.P., 2006. Connections of the subiculum of the rat: topography in relation to co- 1428
lumnar and laminar organization. *Behav. Brain Res.* 174, 251–264. 1429
- Wright, N.F., Vann, S.D., Erichsen, J.T., O'Mara, S.M., Aggleton, J.P., 2013. Segregation of 1430
parallel inputs to the anteromedial and anteroventral thalamic nuclei of the rat. 1431
J. Comp. Neurol. 521, 2966–2986. 1432

1433